

Diffraction DIS Cross Sections and Parton Distributions from Rapidity Gap and Leading Proton Data



Frank-Peter Schilling (CERN)



2006 HERA-LHC Workshop
CERN, June 7th, 2006

Outline:

- hep-ex/0606003
- hep-ex/0606004

HERA AND THE LHC
2nd workshop on the implications of HERA for LHC physics

6-9 June 2006
CERN, Geneva

Parton density functions
Multijet final states and energy flow
Heavy quarks
Diffraction
Monte Carlo tools

Organising Committee:
G. Altarelli (CERN), J. Blümlein (DESY),
M. Botje (NIKHEF), J. Butterworth (UCL),
A. De Roeck (CERN) (chair), K. Eggert (CERN),
E. Gallo (INFN), H. Jung (DESY) (chair),
M. Klein (DESY), M. Mangano (CERN),
A. Morech (CERN), G. Polesello (INFN),
O. Schneider (EPFL), R. Yoshida (ANL)

Auditory Committee:
J. Bartels (Hamburg), M. Della Negra (CERN),
J. Ellis (CERN), J. Engelen (CERN),
G. Gustafson (Lund), G. Ingelman (Uppsala),
P. Jenni (CERN), R. Klanner (DESY),
L. McLerran (BNL), T. Nakada (CERN),
D. Schlatter (CERN), F. Schrempff (DESY),
J. Schukraft (CERN), J. Stirling (Durham),
W.K. Tang (Michigan State), A. Wagner (DESY),
R. Yoshida (ANL)

www.desy.de/~heralhc heralhc.workshop@cern.ch

Final Results from two Publications

DESY 06-049
May 2006

ISSN 0418-9833

Measurement and QCD Analysis of the Diffractive Deep-Inelastic Scattering Cross Section at HERA

H1 Collaboration

DESY 06-049, hep-ex/0606004

Abstract

A detailed analysis is presented of the diffractive deep-inelastic scattering process $ep \rightarrow eXY$, where Y is a proton or a low mass proton excitation carrying a fraction $1-x_p > 0.95$ of the incident proton longitudinal momentum and the squared four-momentum transfer at the proton vertex satisfies $|t| < 1 \text{ GeV}^2$. Using data taken by the H1 experiment, the cross section is measured for photon virtualities in the range $3.5 \leq Q^2 \leq 1600 \text{ GeV}^2$, triple differentially in x_p , Q^2 and $\beta = z/x_p$, where x is the Bjorken scaling variable. At low x_p , the data are consistent with a factorisable x_p dependence, which can be described by the exchange of an effective pomeron trajectory with intercept $\alpha_p(0) = 1.118 \pm 0.008$ (exp.) $^{+0.029}_{-0.010}$ (model). Diffractive parton distribution functions and their uncertainties are determined from a next-to-leading order DGLAP QCD analysis of the Q^2 and β dependences of the cross section. The resulting gluon distribution carries an integrated fraction of around 70% of the exchanged momentum in the Q^2 range studied. Total and differential cross sections are also measured for the diffractive charged current process $e^+p \rightarrow \nu_e XY$ and are found to be well described by predictions based on the diffractive parton distributions. The ratio of the diffractive to the inclusive neutral current ep cross sections is studied. Over most of the kinematic range, this ratio shows no significant dependence on Q^2 at fixed x_p and β or on x at fixed Q^2 and β .

Submitted to *Eur. Phys. J. C*

arXiv:hep-ex/0606004 v1 1 Jun 2006

DESY 06-048
May 2006

ISSN 0418-9833

Diffractive Deep-Inelastic Scattering with a Leading Proton at HERA

H1 Collaboration

DESY 06-048, hep-ex/0606003

Abstract

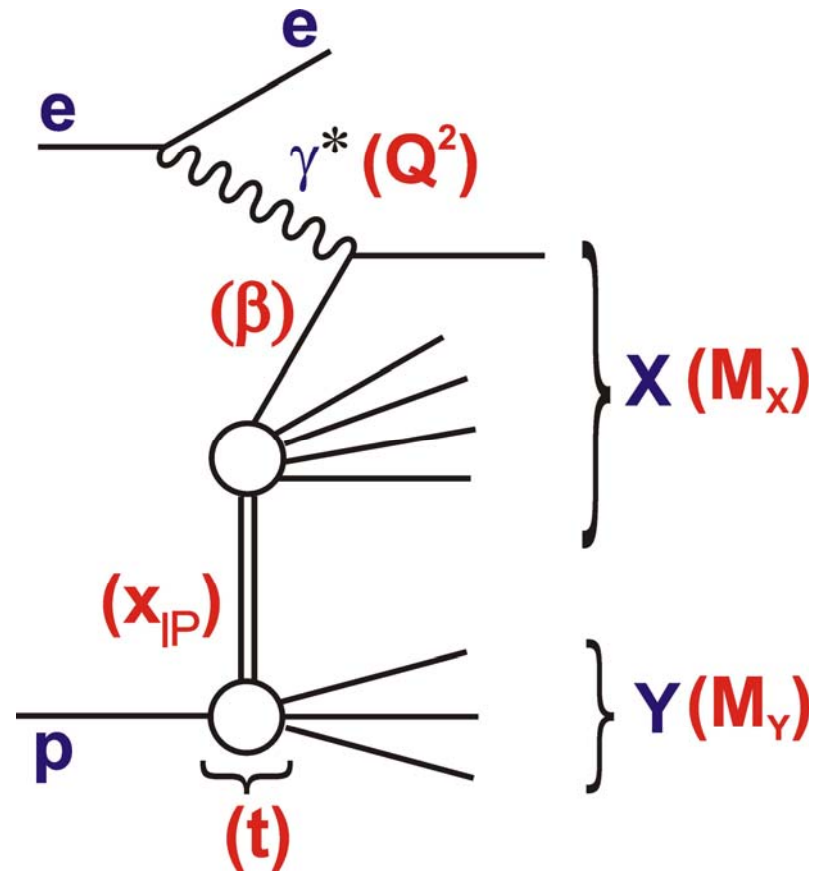
The cross section for the diffractive deep-inelastic scattering process $ep \rightarrow eXp$ is measured, with the leading final state proton detected in the H1 Forward Proton Spectrometer. The data analysed cover the range $x_p < 0.1$ in fractional proton longitudinal momentum loss, $0.08 < |t| < 0.5 \text{ GeV}^2$ in squared four-momentum transfer at the proton vertex, $2 < Q^2 < 50 \text{ GeV}^2$ in photon virtuality and $0.004 < \beta = z/x_p < 1$, where x is the Bjorken scaling variable. For $x_p \lesssim 10^{-2}$, the differential cross section has a dependence of approximately $d\sigma/dt \propto e^{6t}$, independently of x_p , β and Q^2 within uncertainties. The cross section is also measured triple differentially in x_p , β and Q^2 . The x_p dependence is interpreted in terms of an effective pomeron trajectory with intercept $\alpha_p(0) = 1.114 \pm 0.018$ (stat.) ± 0.012 (syst.) $^{+0.040}_{-0.020}$ (model) and a sub-leading exchange. The data are in good agreement with an H1 measurement for which the event selection is based on a large gap in the rapidity distribution of the final state hadrons, after accounting for proton dissociation contributions in the latter. Within uncertainties, the dependence of the cross section on x and Q^2 can thus be factorised from the dependences on all studied variables which characterise the proton vertex, for both the pomeron and the sub-leading exchange.

Submitted to *Eur. Phys. J. C*

arXiv:hep-ex/0606003 v1 1 Jun 2006

Contents

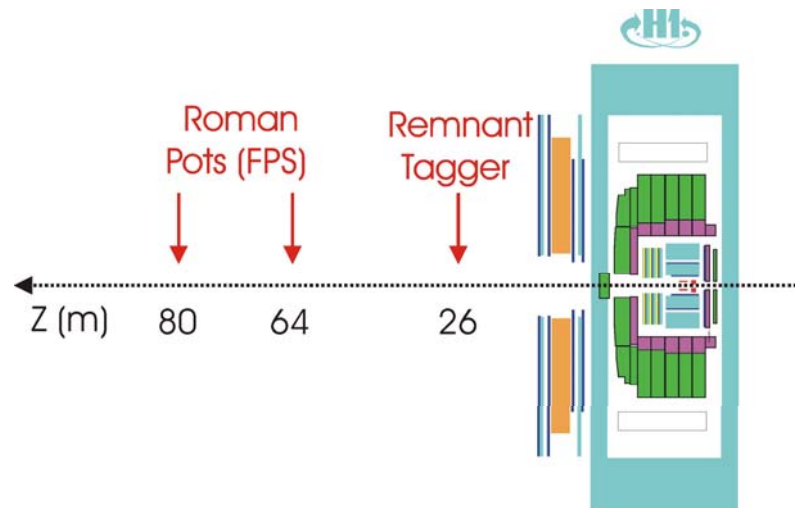
- Comparison between leading proton and rapidity gap data
- Dependences on t
- Q^2 and β dependences and NLO DGLAP QCD fits
- x_{IP} dependences and $\alpha_{IP}(0)$
- First measurement of charged current diffraction
- Comparisons between diffractive and inclusive DIS cross sections



Event Selection Methods

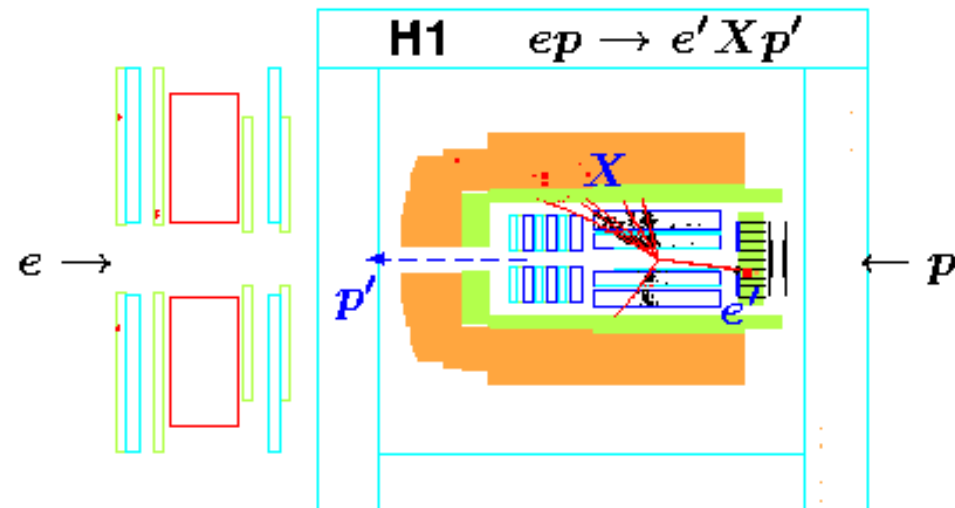
1. Tag and measure final state proton in Forward Proton Spectrometer (FPS method)

- ❑ No proton dissociation
- ❑ Can measure t
- ❑ Acceptance at high x_{IP}
- ❑ ... but low Pot acceptance



2. Require Large Rapidity Gap spanning at least $3.3 < \eta < 7.5$ and measure hadrons in central detector (LRG method)

- ❑ Some proton dissociation
- ❑ Correct to $M_Y < 1.6$ GeV
- ❑ Near-perfect acceptance at low x_{IP}



Data Sets and Observables

- **FPS data sample**

- 1999-2000 data (28 pb⁻¹)

- **Study of t dependence:**

$$x_{\mathbb{P}} \frac{d^2 \sigma^{ep \rightarrow eXp}}{dx_{\mathbb{P}} dt}$$

- **The Diffractive reduced cross section:**

$$\frac{d^4 \sigma^{ep \rightarrow eXp}}{dx dQ^2 dx_{\mathbb{P}} dt} = \frac{4\pi\alpha^2}{xQ^4} Y_+ \sigma_r^{D(4)}(x, Q^2, x_{\mathbb{P}}, t)$$

- **Relates to the structure functions F_2^D and F_L^D as:**

$$\sigma_r^{D(4)}(x, Q^2, x_{\mathbb{P}}, t) = F_2^{D(4)} - \frac{y^2}{Y_+} F_L^{D(4)} \approx F_2^{D(4)}$$

- **Integrated over t:**

$$\sigma_r^{D(3)}(x, Q^2, x_{\mathbb{P}}) = \int_{-1}^{t_{min}} \sigma_r^{D(4)}(x, Q^2, x_{\mathbb{P}}, t) dt$$

- **LRG data sample**

- 1997 data (2 pb⁻¹, Q²<13.5 GeV²)

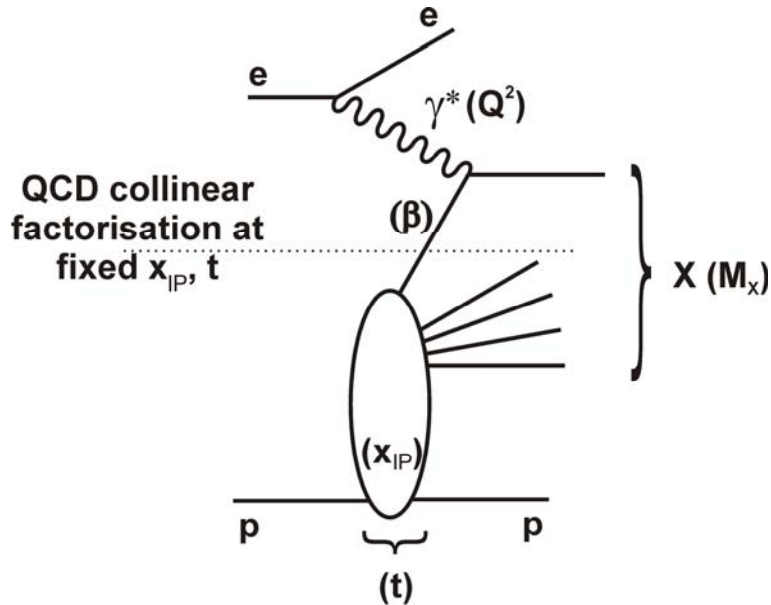
- 1997 data (11 pb⁻¹, 13.5<Q²<105 GeV²)

- 99-00 data (62 pb⁻¹, Q²>133 GeV²)

Two Levels of Factorization

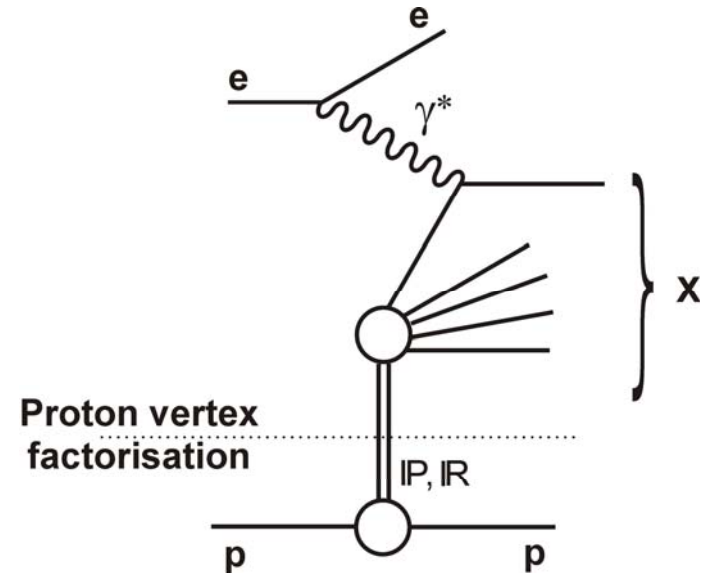
- QCD hard scattering collinear factorization (Collins) at fixed x_{IP} and t

- After integration over measured M_Y, t ranges



- “Proton vertex” factorization of x, Q^2 from x_{IP}, t (and M_Y) dependences

- Separately for leading IP and sub-leading IR exchanges

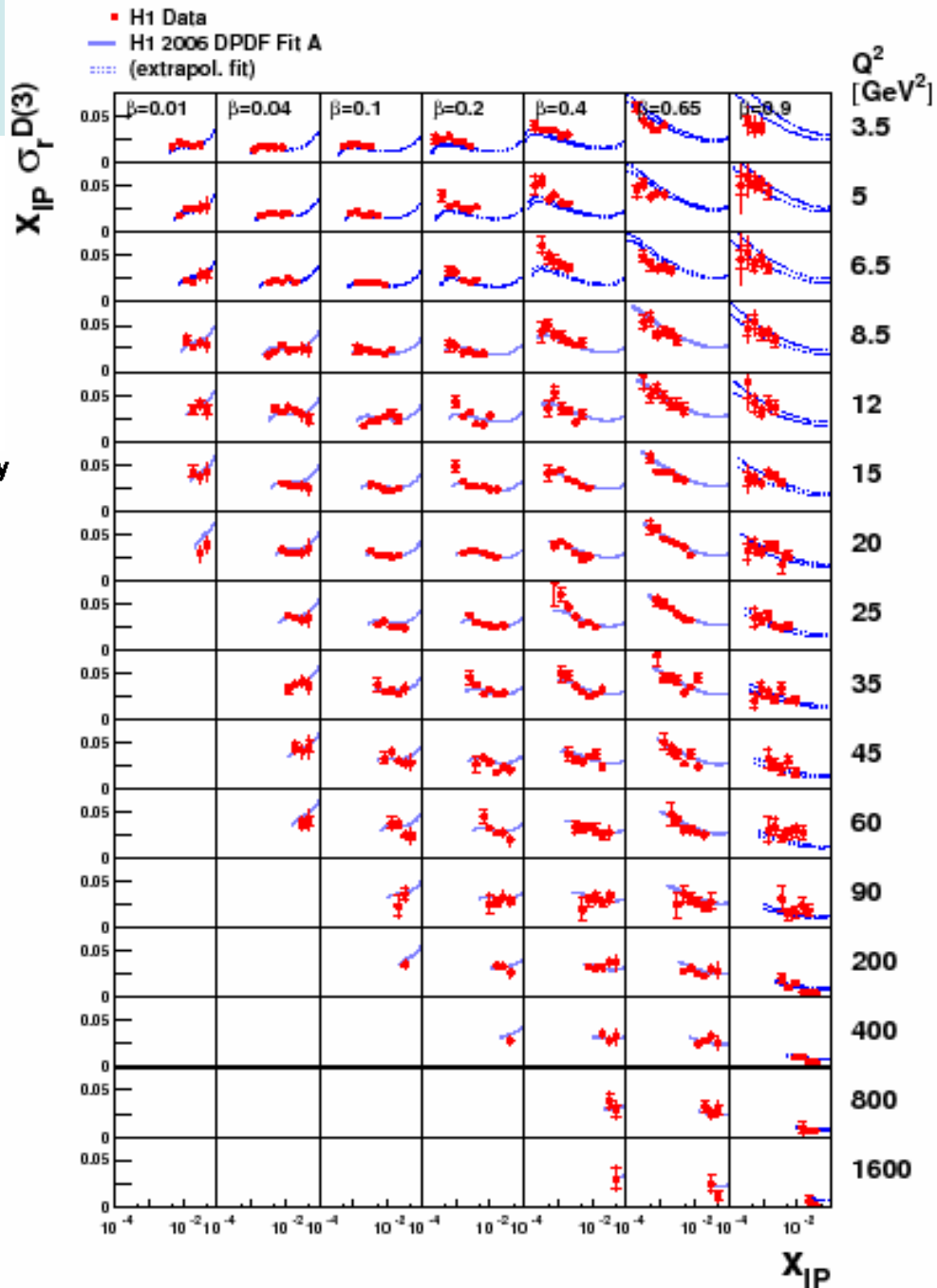
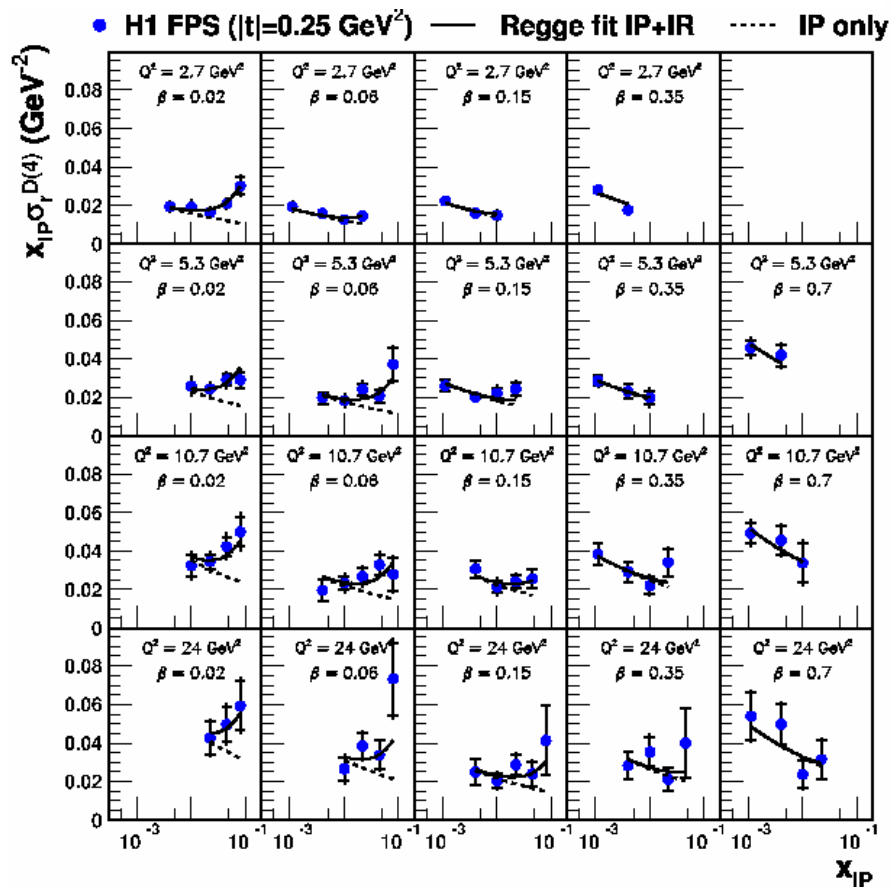


$$d\sigma_i(ep \rightarrow eXY) = f_i^D(x, Q^2, x_{IP}, t) \otimes d\hat{\sigma}^{ei}(x, Q^2)$$

$$f_i^D(x, Q^2, x_{IP}, t) = f_{IP/p}(x_{IP}, t) \times f_i^{IP}(\beta = x/x_{IP}, Q^2)$$

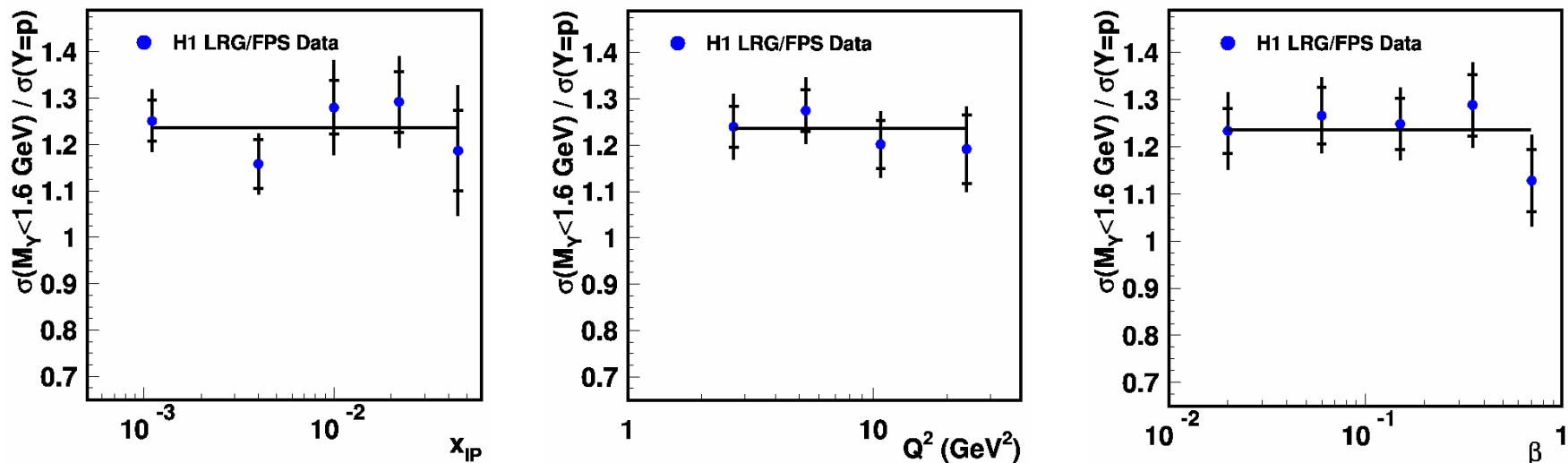
Data Overview

- **LRG: $M_Y < 1.6$ GeV**
 \square $3.5 < Q^2 < 1600$ GeV²
- **FPS: $Y=p$**
 \square $2.7 < Q^2 < 24$ GeV²



Comparison LRG vs FPS Data

- Form ratio LRG/FPS of measurements as function of x_{IP} , β or Q^2 after integration over others



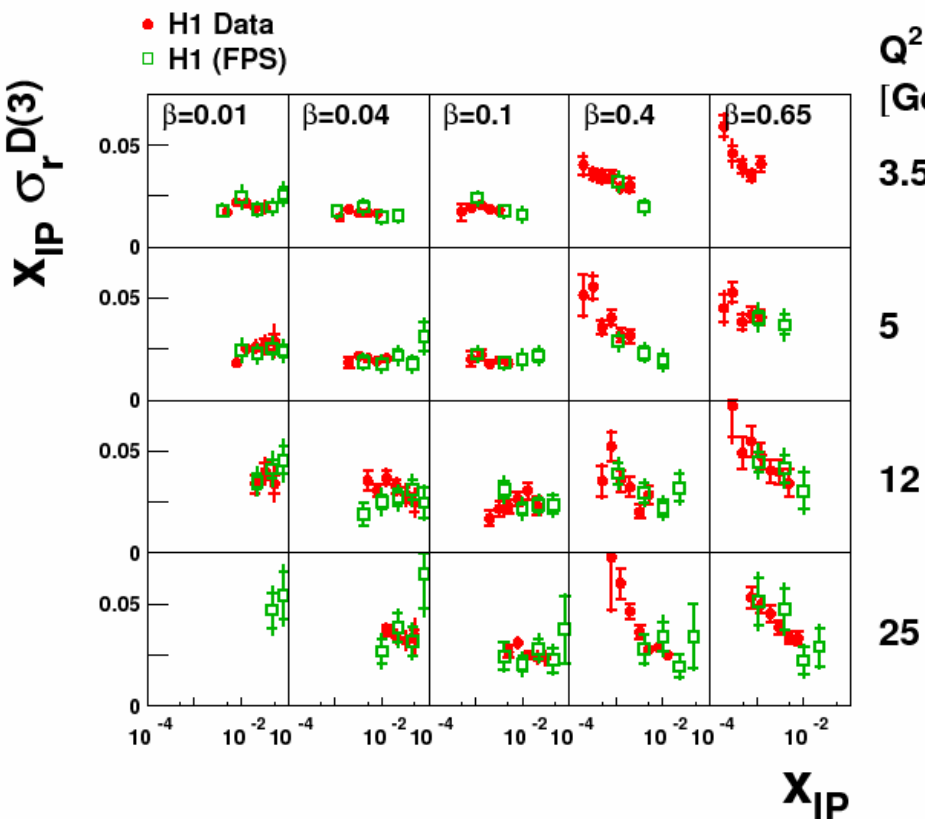
□ Independent of kinematics within errors

$$\frac{\sigma(M_Y < 1.6 \text{ GeV})}{\sigma(Y = p)} = 1.23 \pm 0.03(\text{stat.}) \pm 0.16(\text{syst.})$$

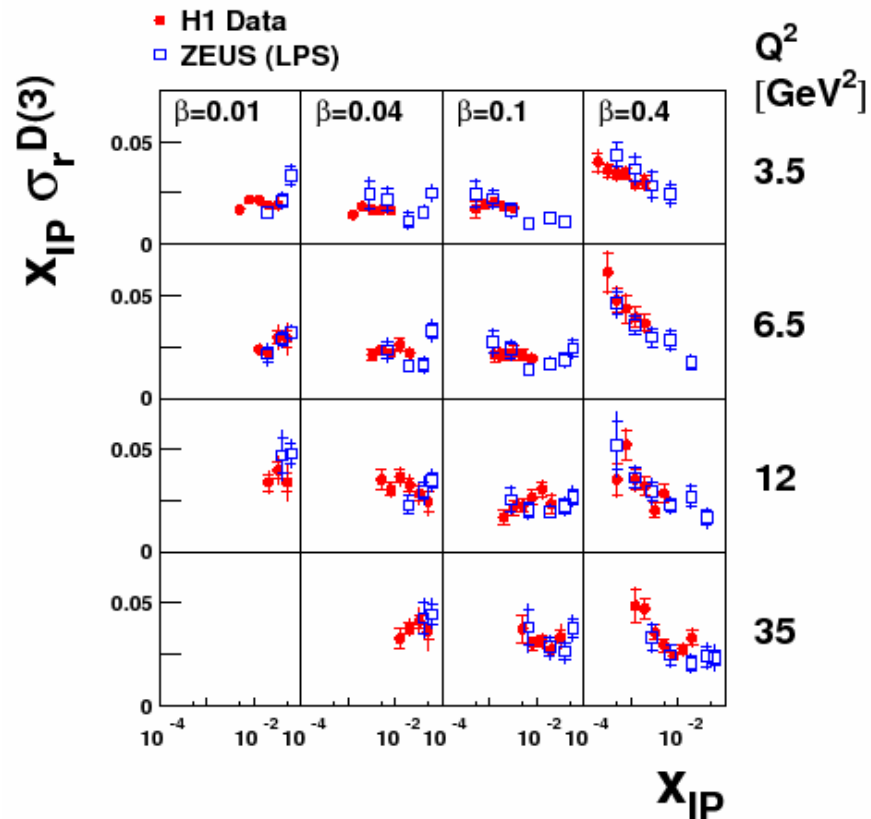
- Agreement in detail between methods
- M_Y dependence factorizes within (10% non-normalization) errors!

Comparison of H1-LRG with H1-FPS and ZEUS-LPS data

• LRG vs FPS data:



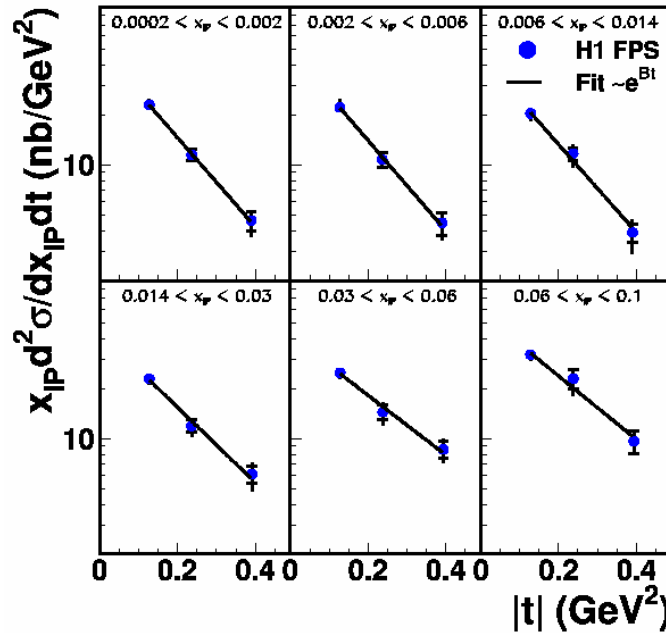
• LRG vs ZEUS LPS data:



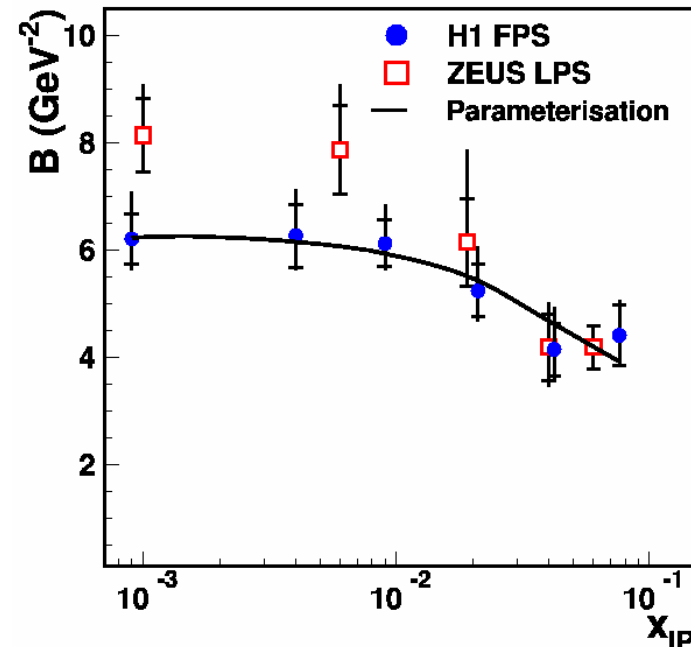
- FPS and ZEUS-LPS data scaled by global factor of 1.23
- ZEUS-LPS and H1-FPS normalizations agree to 8%
- Very good agreement between proton tagging and LRG methods if p dissociation is accounted for!

t dependence from FPS measurements

- Fit to $\exp(Bt)$ in bins of x_{IP}



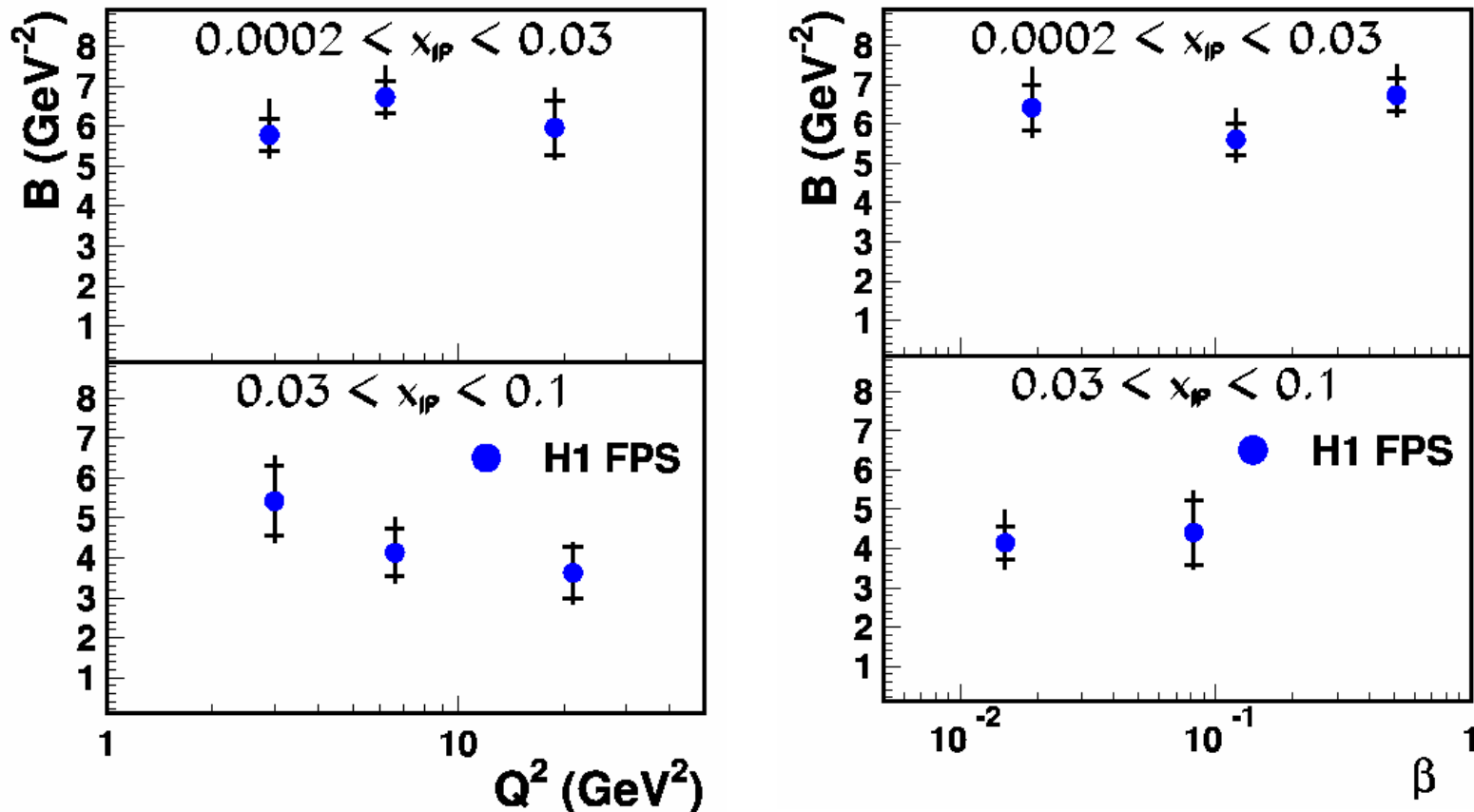
- Resulting $B(x_{IP})$



- $B(x_{IP})$ data constrain IP,IR flux factors in p vertex fact. Model
- Regge motivated form: $f_{IP/p}(x_{IP}, t) = \frac{e^{B_{IP}t}}{x_{IP}^{2\alpha_{IP}(t)-1}}$ $\alpha_{IP}(t) = \alpha_{IP}(0) + \alpha'_{IP}t$
- E.g. fitting low x_{IP} data to $B = B_{IP} + 2\alpha'_{IP} \ln(1/x_{IP})$ yields $B_{IP} = 5.5_{-0.7}^{+2.0} \text{ GeV}^{-2}$ $\alpha'_{IP} = 0.06_{-0.06}^{+0.19} \text{ GeV}^{-2}$

t-slope dependence on β or Q^2 ?

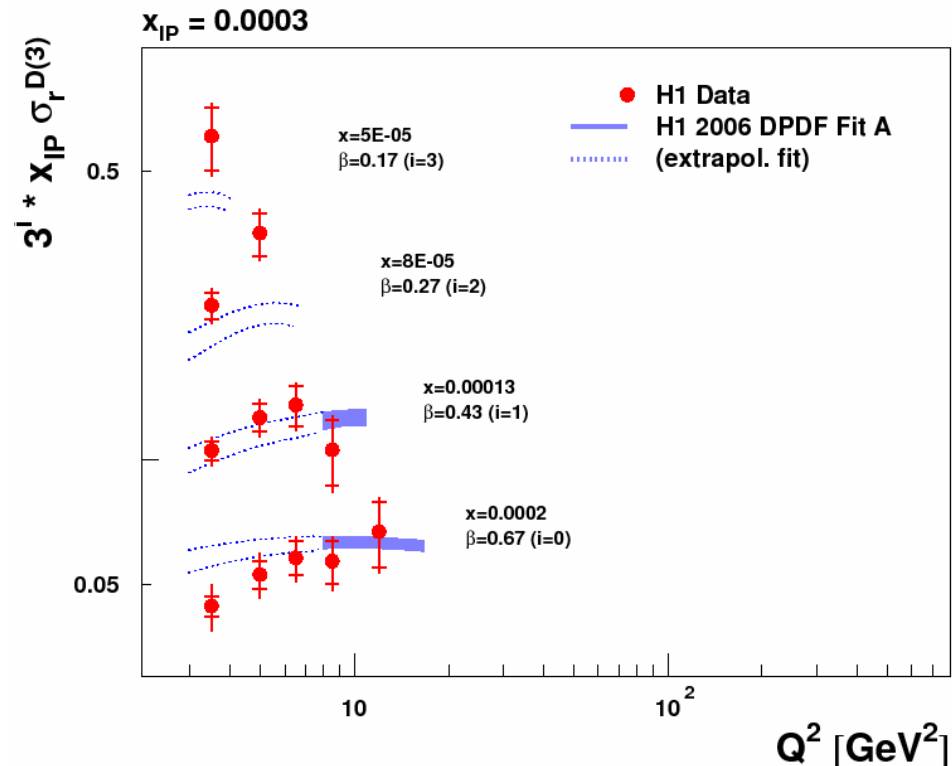
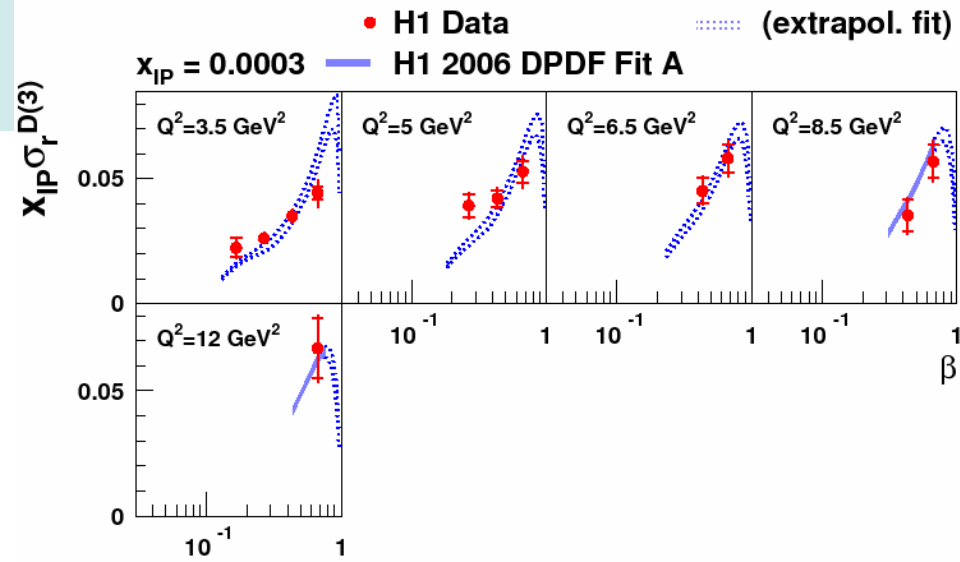
- B measured double differentially in (β or Q^2) and x_{IP}**



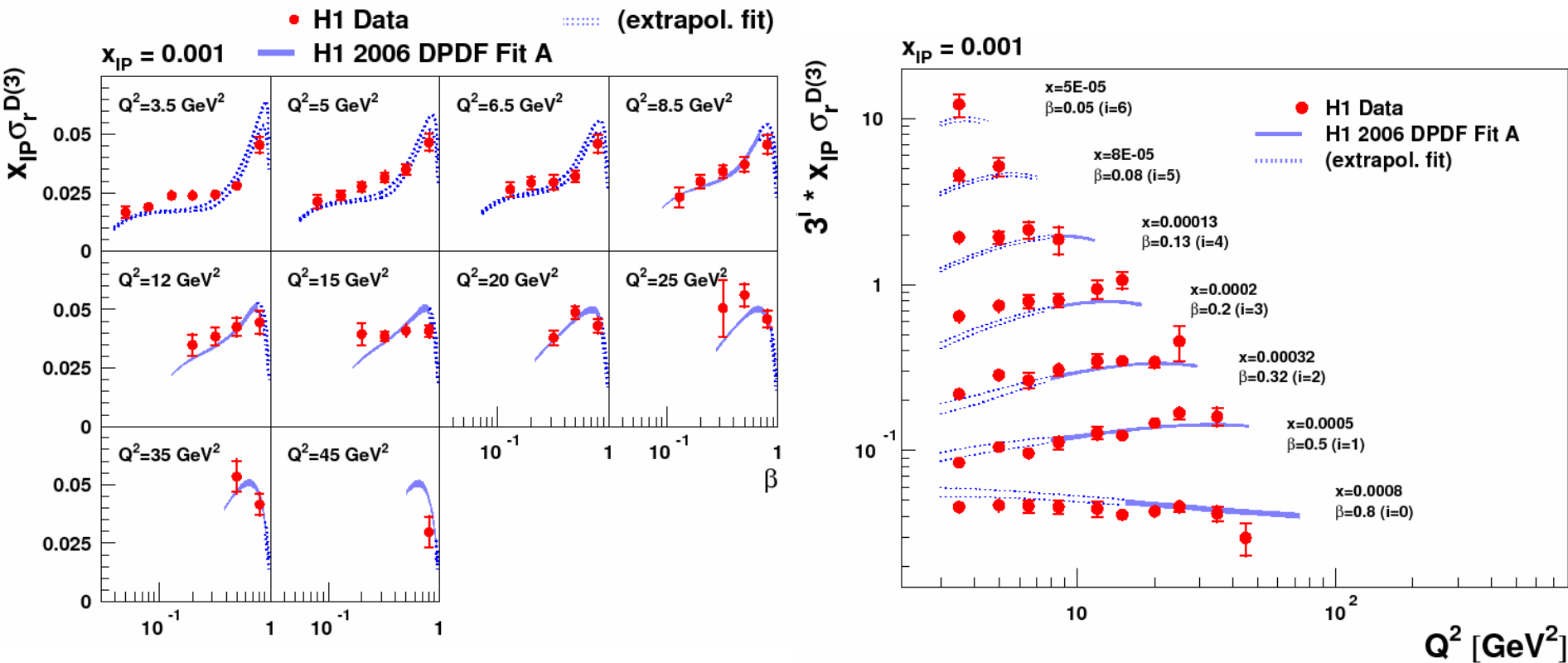
- No change of t dependence with β or Q^2 at fixed x_{IP}**
- Proton vertex factorization for t dependence working within errors**

$\sigma_r^{D(3)}(\beta, Q^2, x_{IP})$ at $x_{IP}=0.0003$

- Principal binning scheme for **LRG data**
- Study Q^2 and x ($=\beta * x_{IP}$) dependences in detail at small number of fixed x_{IP} values
- Good precision – in best regions **5% (stat.)**, **5% (syst.)**, **6% (norm.)**
- Directly measures diffractive quark density at fixed x_{IP}
- Data compared with “**H1 2006 DPDF fit**” and its error band (assumes p vtx factorization, see later)

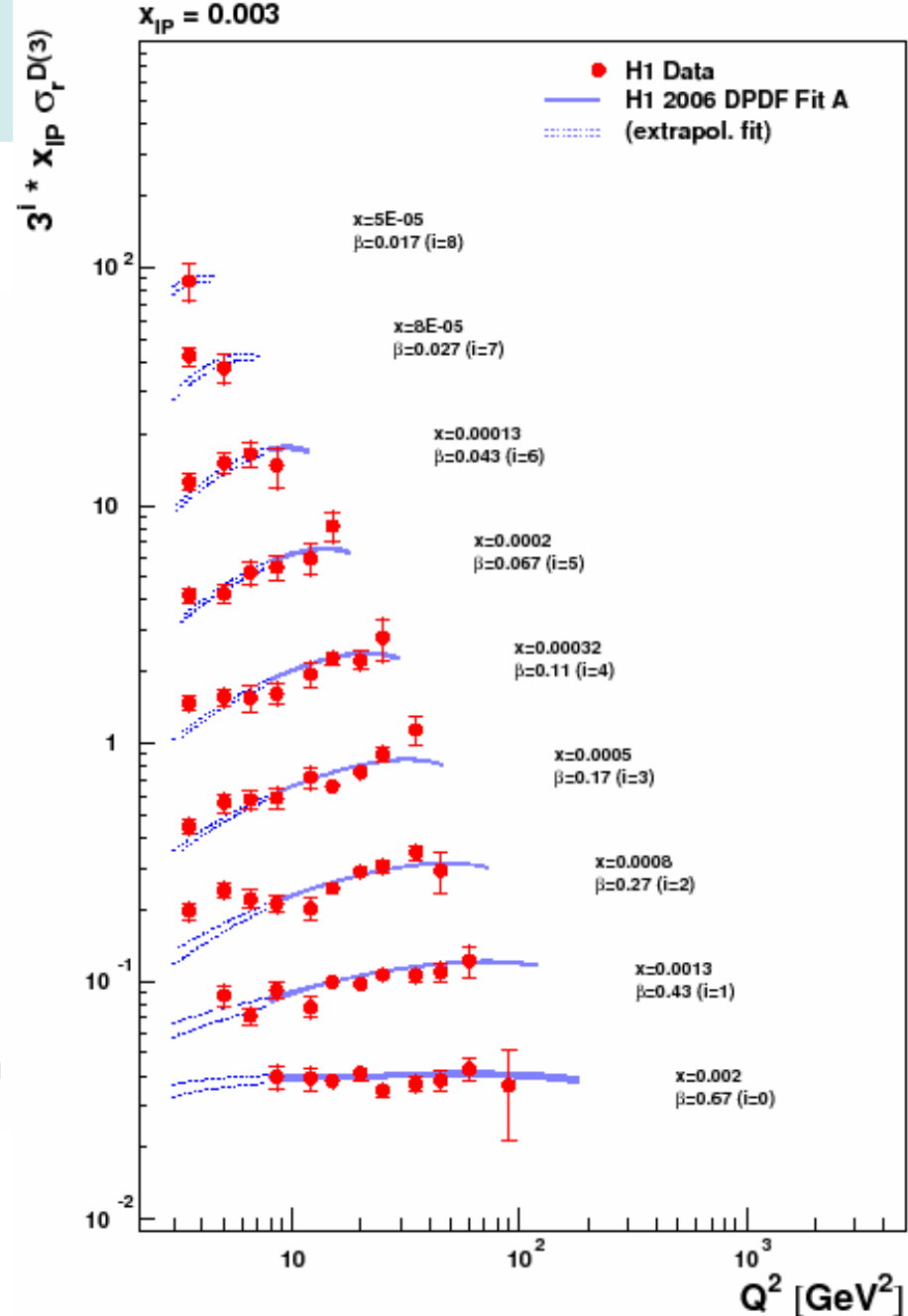
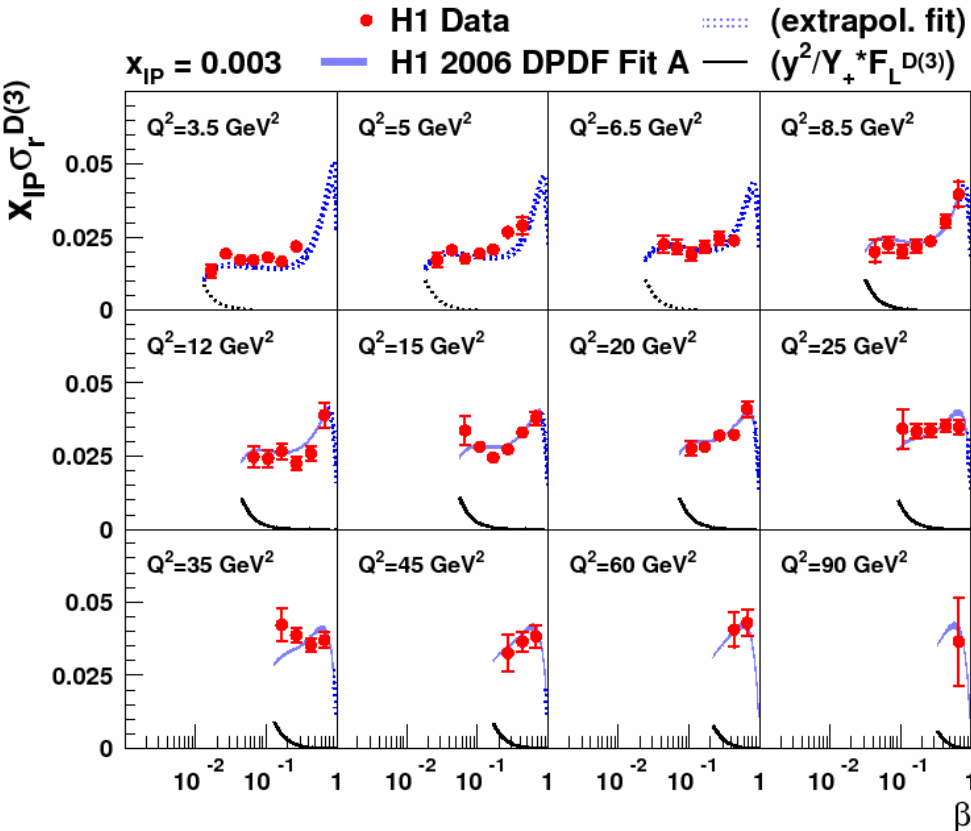


$\sigma_r^{D(3)}(\beta, Q^2, x_{IP})$ at $x_{IP}=0.001$

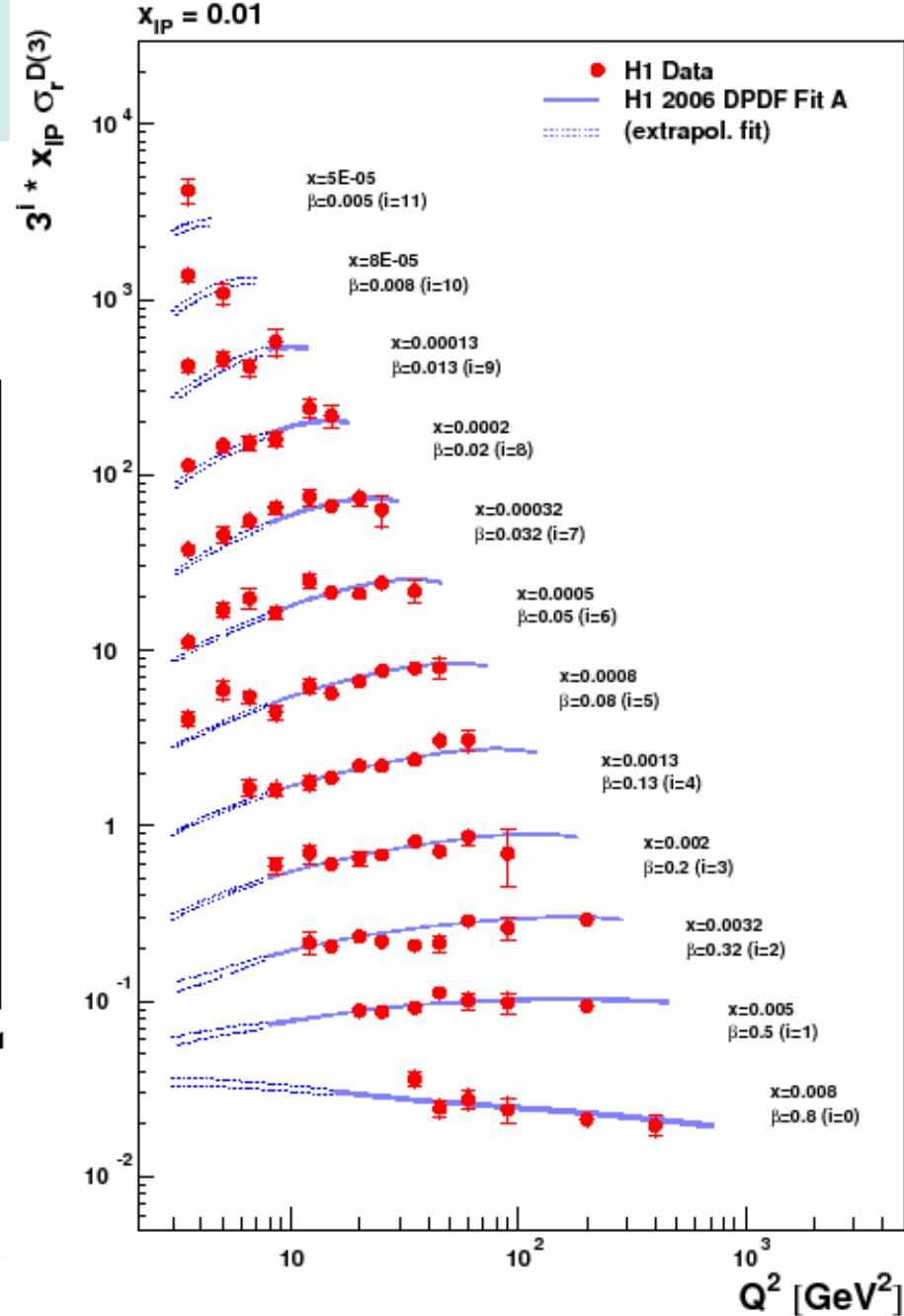
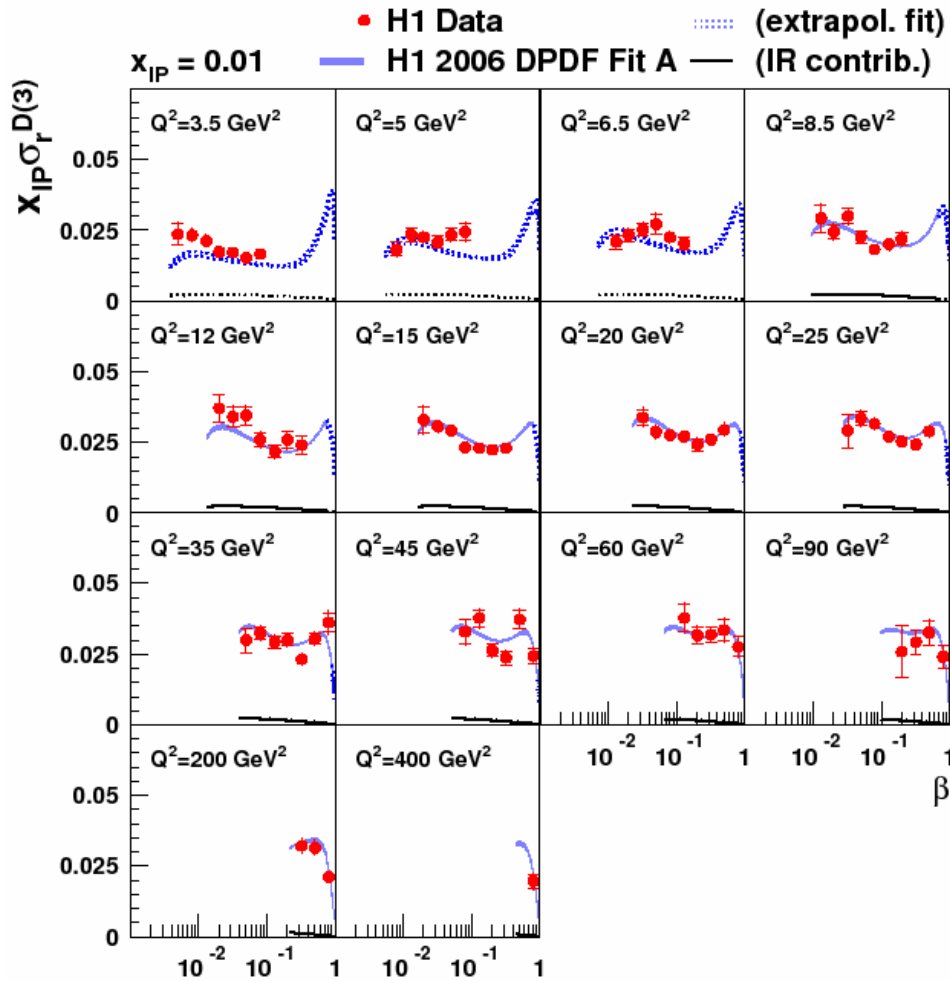


- Like an inclusive F_2 measurement at each value of x_{IP} ...

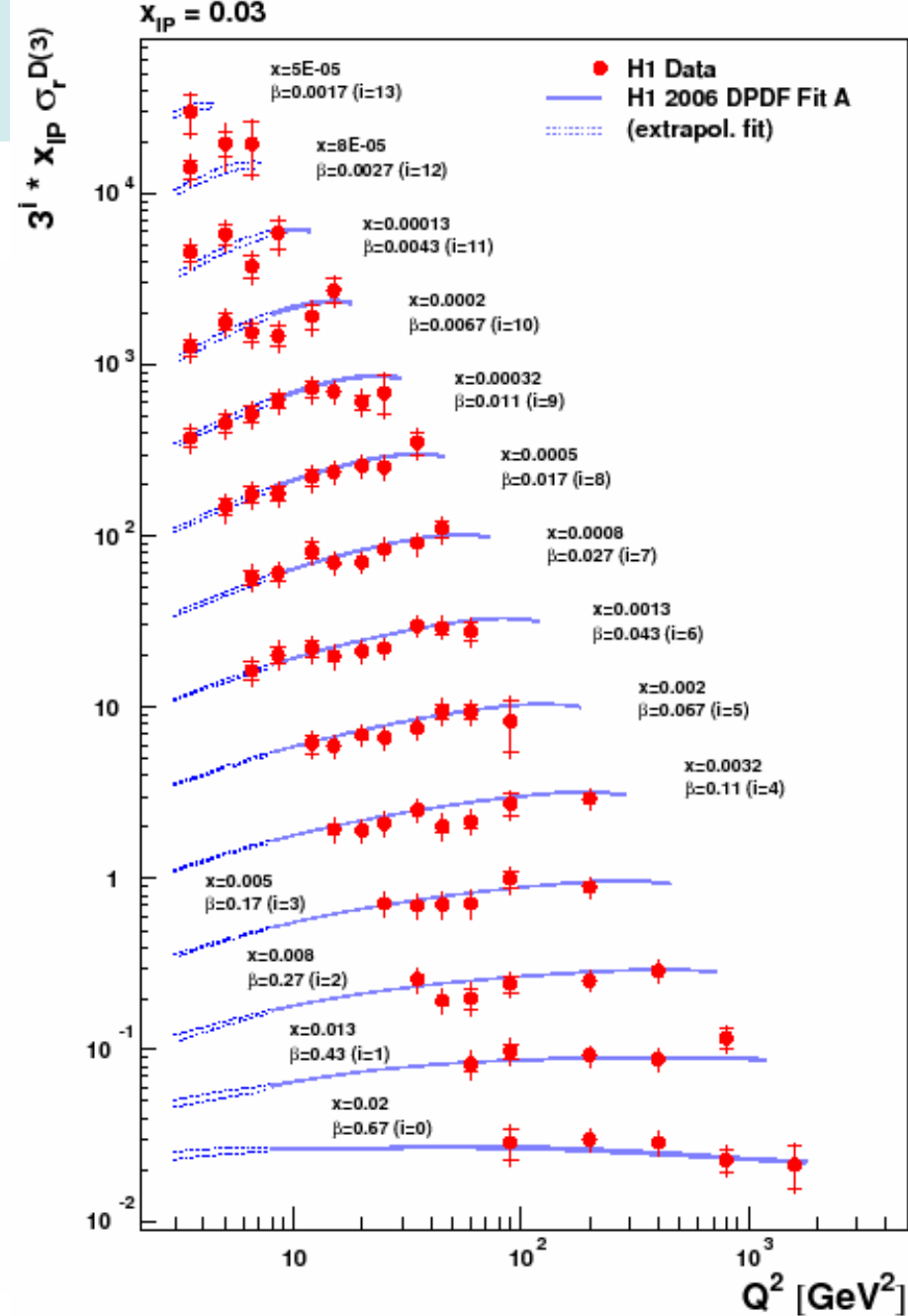
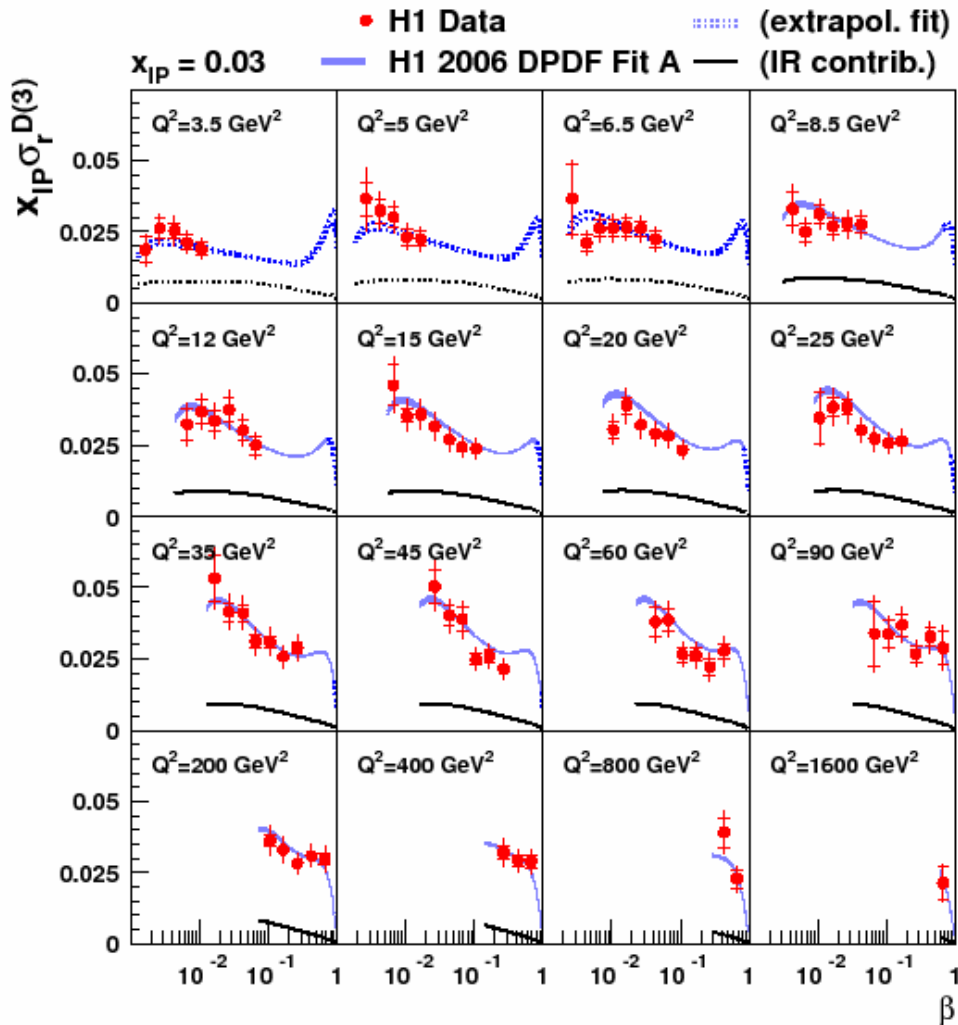
$\sigma_r^{D(3)}(\beta, Q^2, x_{IP})$ at $x_{IP}=0.003$



$\sigma_r^{D(3)}(\beta, Q^2, x_{IP})$ at $x_{IP}=0.01$

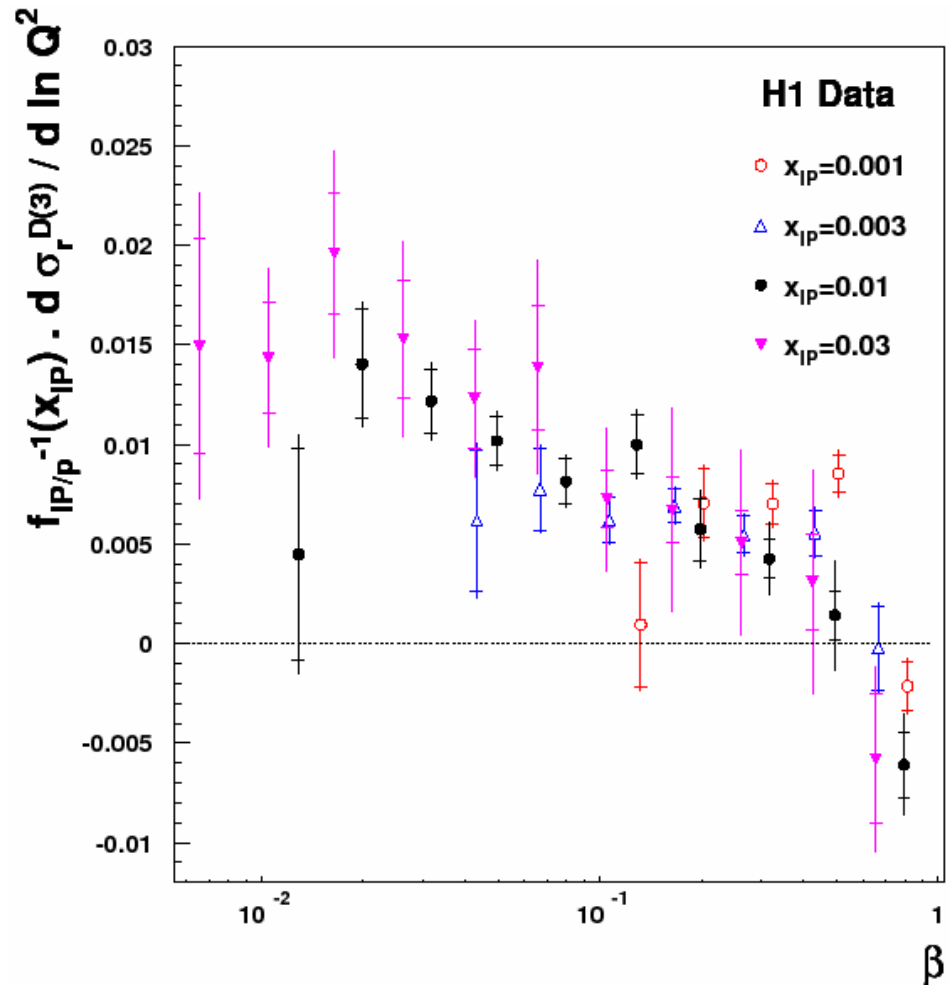


$\sigma_r^{D(3)}(\beta, Q^2, x_{IP})$ at $x_{IP}=0.03$



Q^2 dependence in more detail

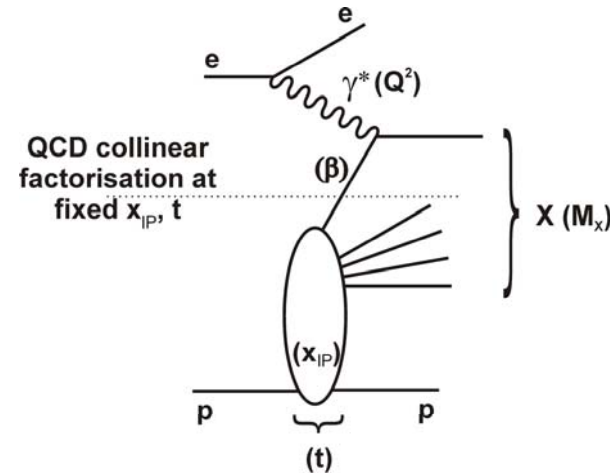
- $\sigma_r^{D(3)}$ measures diffractive quark density
- Its dependence on Q^2 is sensitive to diffractive gluon density
- Fit data at fixed (x, x_{IP}) to $\sigma_r^D = A + B \ln Q^2$, so that $B = d\sigma_r^D / d \ln Q^2$
- Divide results by $f_{IP/p}(x_{IP})$ to compare different x_{IP} values



- Derivatives large and positive at low β
- Suggests large gluon density (independent of x_{IP} within errors)

H1 2006 DPDF fit: Overview

- Fit LRG data from fixed x_{IP} binning, using NLO DGLAP evolution of DPDFs (massive scheme) to describe x, Q^2 dependences
- Proton vtx factorisation framework (supported by data)
 - ❑ relate data from different x_{IP} values with complementary x, Q^2 coverage
- For **IP exchange**, free parameters are
 - ❑ $\alpha_{IP}(0)$ (describes x_{IP} dependence)
 - ❑ DPDF parameters at evolution starting scale Q_0^2



$$f_{IP/p}(x_{IP}, t) = \frac{e^{B_{IP}t}}{x_{IP}^{2\alpha_{IP}(t)-1}}$$

- For **sub-leading IR**
 - ❑ all flux parameters taken from previous data
 - ❑ PDFs taken from Owens- π ; single free param for normalization

Kinematic range and DPDF parameterization

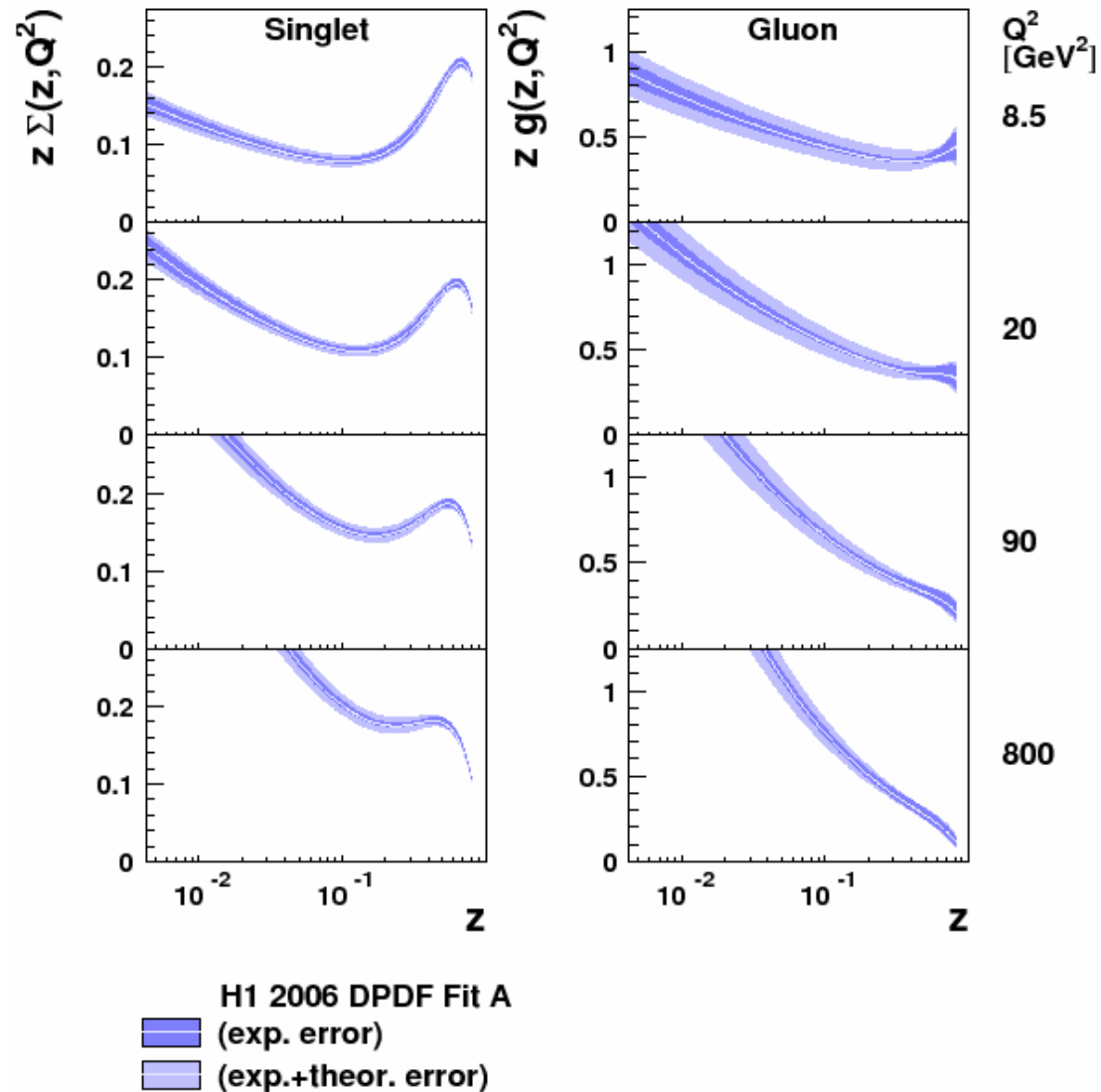
- To ensure data fitted are compatible with chosen framework, test sensitivity of fit results to variations of kinematic boundaries
 - ❑ Results stable for most variations ($\beta_{\max}, \beta_{\min}, M_{X,\min}, x_{IP,\max}$)
 - ❑ Systematic variation of gluon density with minimum Q^2 of data included in fit for $Q^2 < 8.5 \text{ GeV}^2$; stable for larger Q^2 -min
- Fit all LRG data with $Q^2 \geq 8.5 \text{ GeV}^2, M_x > 2 \text{ GeV}, \beta \leq 0.8$
- Parameterize
 - ❑ quark singlet $z\Sigma(z, Q_0^2)$
 - ❑ gluon $zg(z, Q_0^2)$ density

$$z\Sigma(z, Q_0^2) = A_q z^{B_q} (1 - z)^{C_q} \quad zg(z, Q_0^2) = A_g (1 - z)^{C_g}$$

- ❑ Gluon insensitive to B_g
- Small number of parameters
 - ❑ need to optimize Q_0^2 wrt χ^2
- Using world average value for $\alpha_s(M_Z) = 0.118$
- Results reproducible with Chebychev polynomials

H1 2006 DPDF fit results (log z scale)

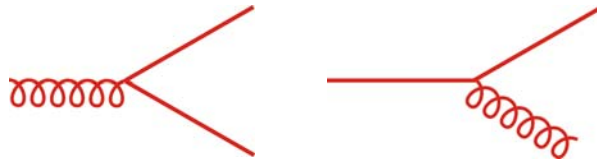
- $Q_0^2 = 1.75 \text{ GeV}^2$
- $\chi^2 \sim 158 / 183 \text{ dof}$
- **Experimental uncertainty obtained by propagating errors on data (c.f. incl. fits, $\Delta\chi^2=1$)**
- **Theoretical uncertainty from varying fixed parameters of fit (flux params, α_s , m_c , m_b etc.) and Q_0^2 ($\Delta\chi^2=1$)**
- **Singlet constrained to $\sim 5\%$, gluon to $\sim 15\%$ at low z; error blowing up at highest z**



A closer look at high z region

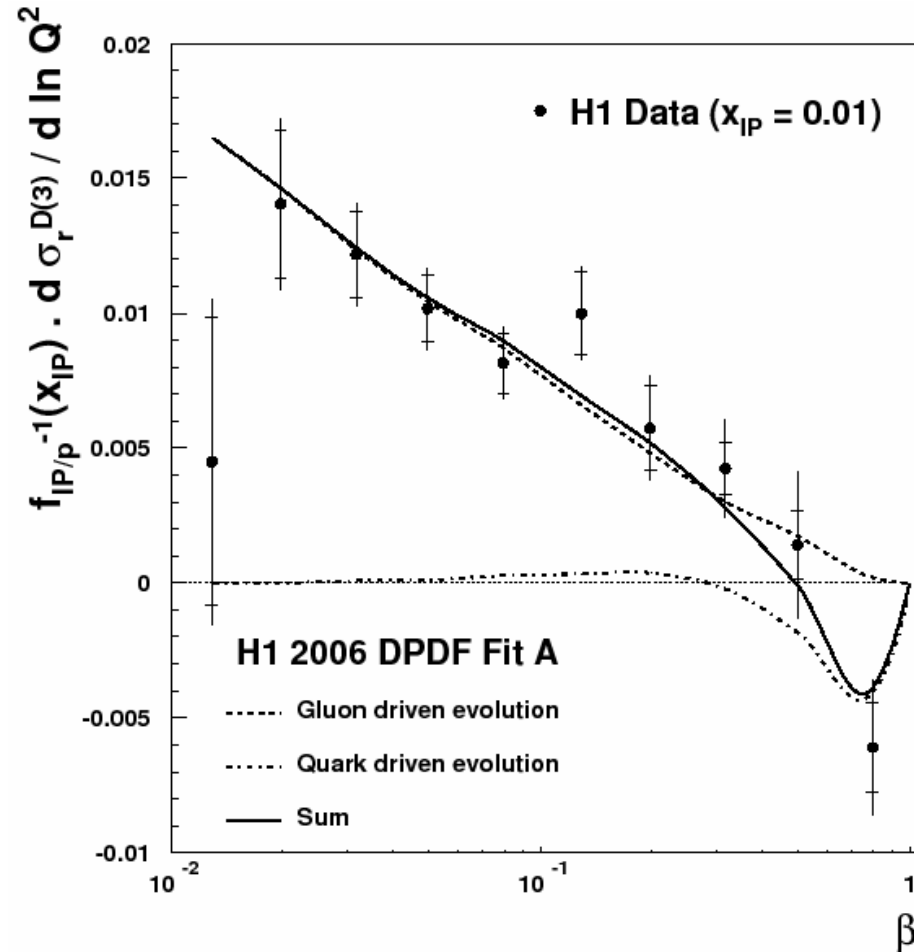
- As there are only singlet quarks, the evolution eq. for F_2^D is

$$\frac{dF_2^D}{d \ln Q^2} \sim \frac{\alpha_s}{2\pi} [P_{qg} \otimes g + P_{qq} \otimes \Sigma]$$



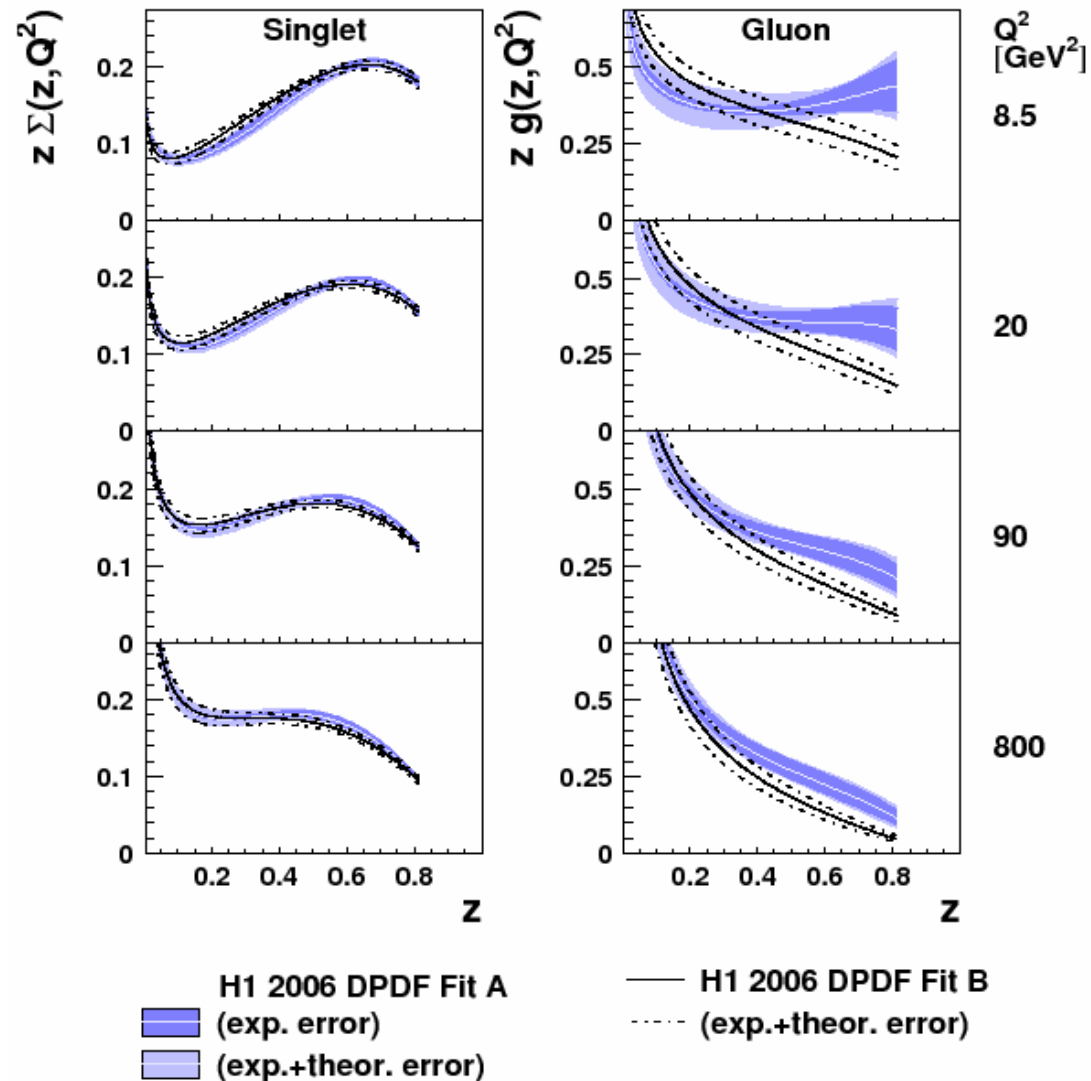
- At low β , evolution driven by $g \rightarrow qq$:
 - strong sensitivity to gluon
- At high β relative error on derivative grows, $q \rightarrow qg$ contribution becomes important:
 - sensitivity to gluon is lost

Log. Derivative wrt Q^2 :



H1 2006 DPDF fit results (lin. z scale)

- Lack of sensitivity to high z gluon confirmed by dropping C_g parameter, so gluon is simple constant at Q_0^2 :
- **Fit B**, $\chi^2 \sim 164/184$ dof
 - ❑ Singlet very stable
 - ❑ Gluon similar at low z
 - ❑ Substantial change to gluon at high z



Effective Pomeron Intercept

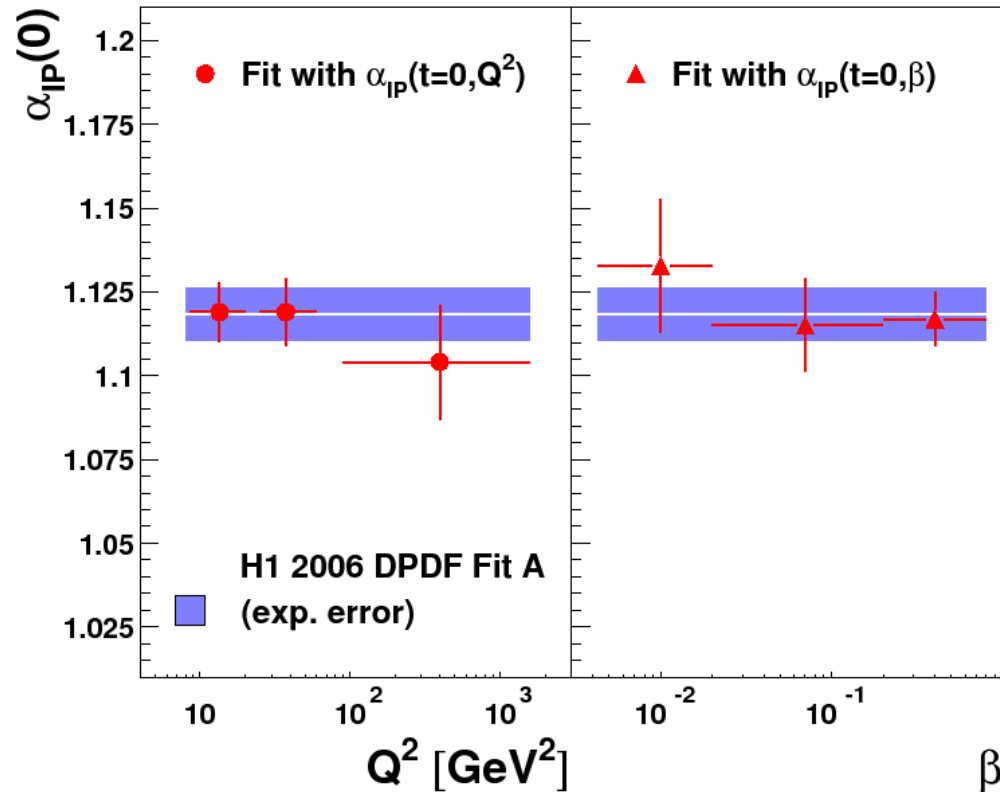
- From QCD fit to LRG data

$$\alpha_{\mathbb{P}}(0) = 1.118 \pm 0.008(\text{exp.})^{+0.029}_{-0.010}(\text{th.})$$

- Dominant uncertainty from strong correlation with $\alpha'_{\mathbb{P}}$: taking $\alpha'_{\mathbb{P}} = 0.25$ instead of 0.06 GeV^{-2} yields $\alpha_{\mathbb{P}}(0) \sim 1.15$

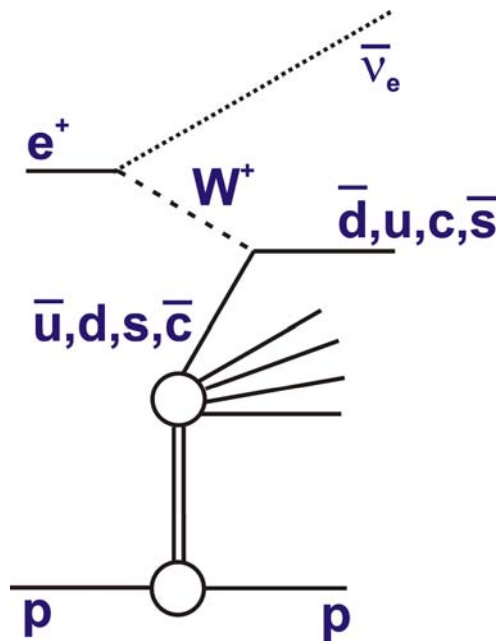
- Stable w.r.t adding extra parameters for $\alpha_{\mathbb{P}}(0)$ in different Q^2 or β regions (consistent with p vtx factorization)

- Consistent result from fits to FPS data:

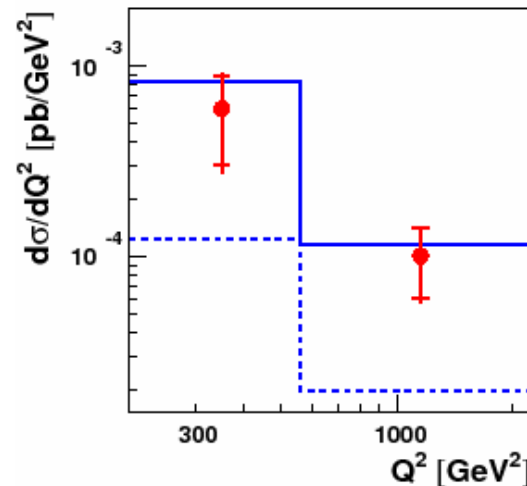
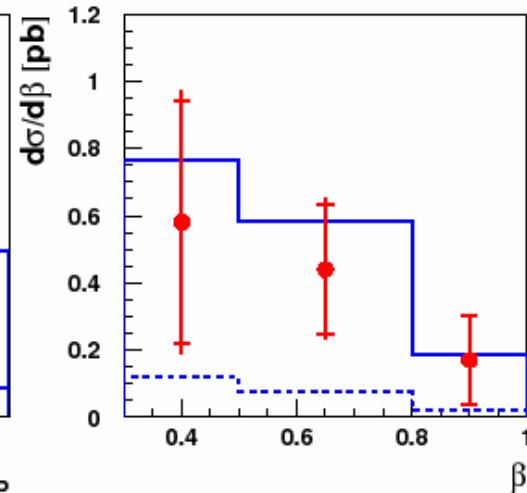
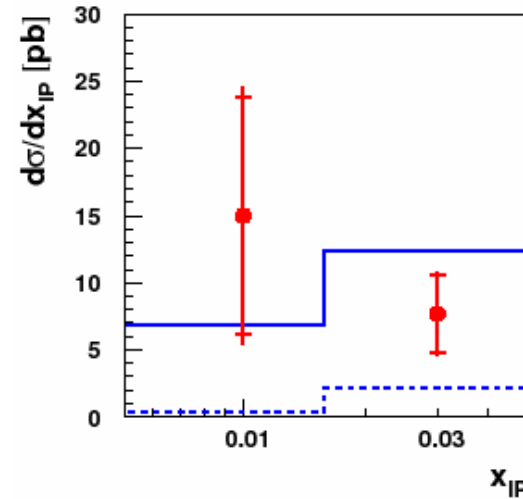


$$\alpha_{\mathbb{P}}(0) = 1.114 \pm 0.018(\text{stat.}) \pm 0.012(\text{syst.})^{+0.040}_{-0.020}(\text{th.})$$

Diffractive Charged Current

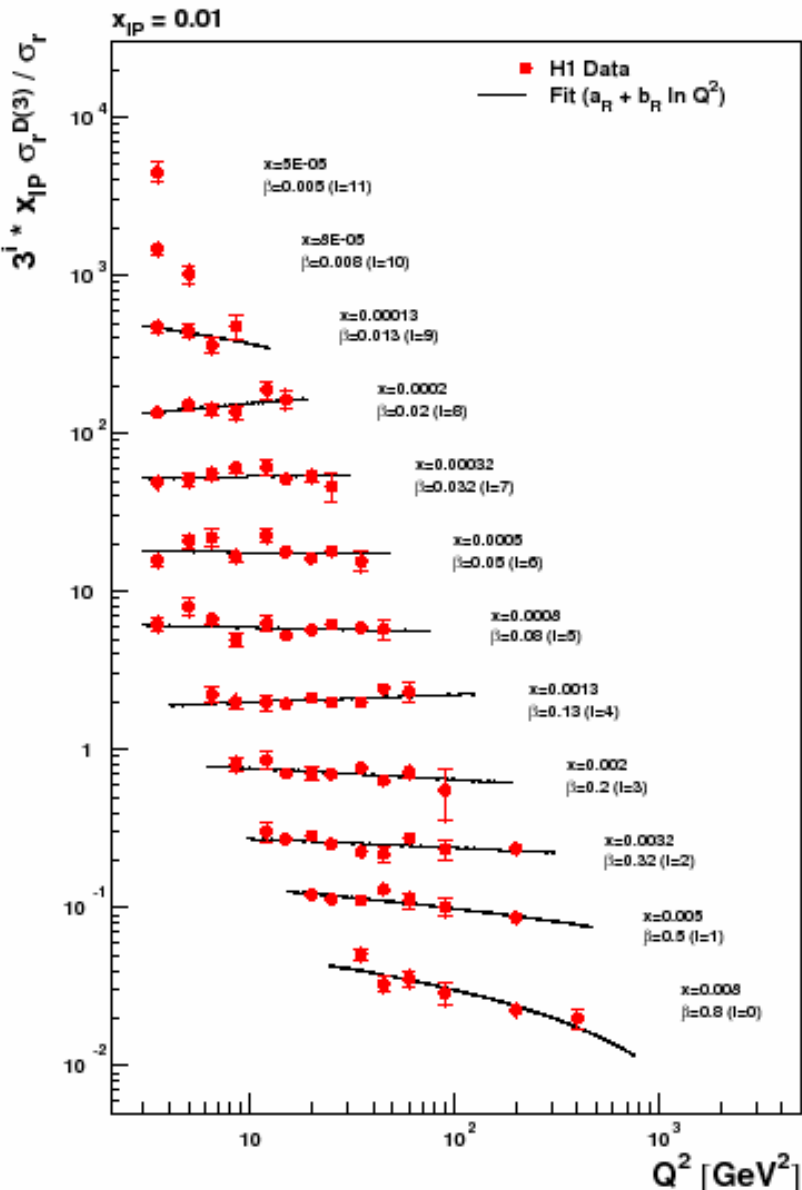


- Sensitive to flavour decomposition of singlet (completely unconstrained by NC data)
- Good agreement with 2006 DPDF fit (assumes $u=d=s=\bar{u}=\bar{d}=\bar{s}$, c from BGF), though statistics very limited so far

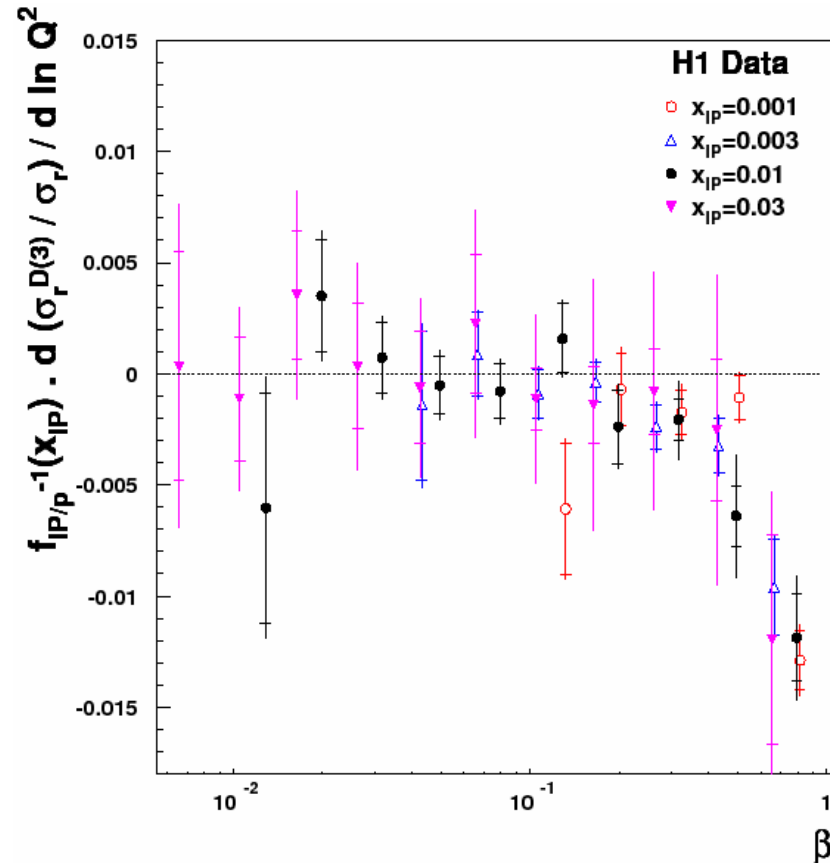


- H1 Data ($Q^2 > 200$ GeV²; $y < 0.9$; $x_{IP} < 0.05$)
- H1 2006 DPDF Fit A
- (IR contrib.)

Ratio diffractive/inclusive: Q^2 dependence



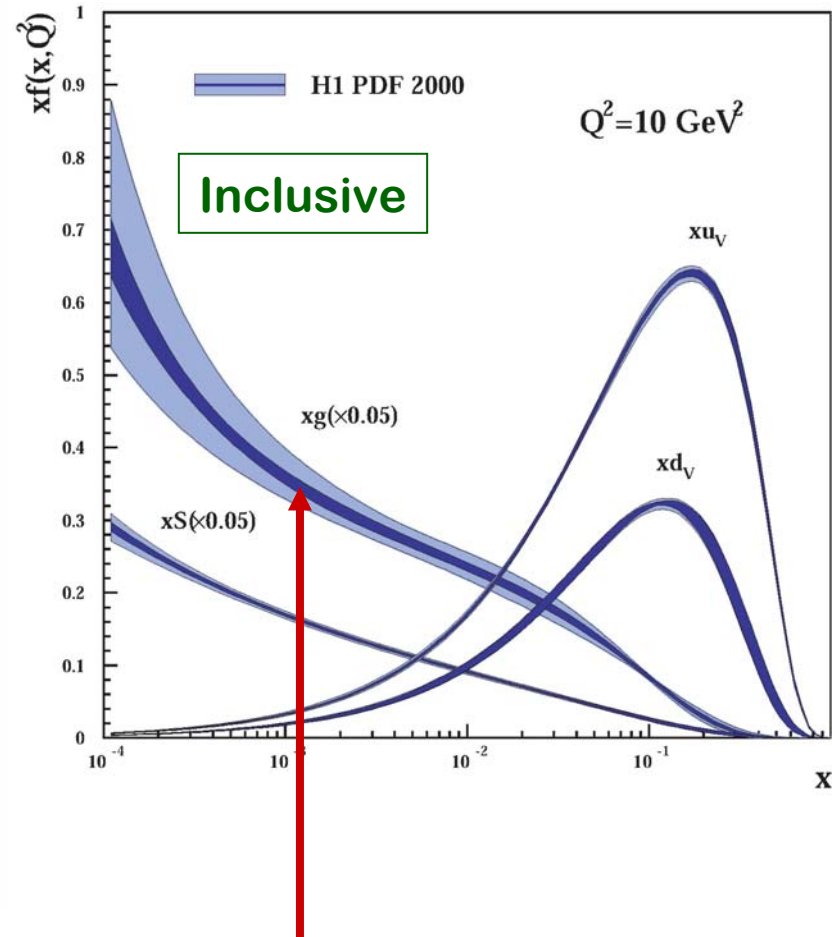
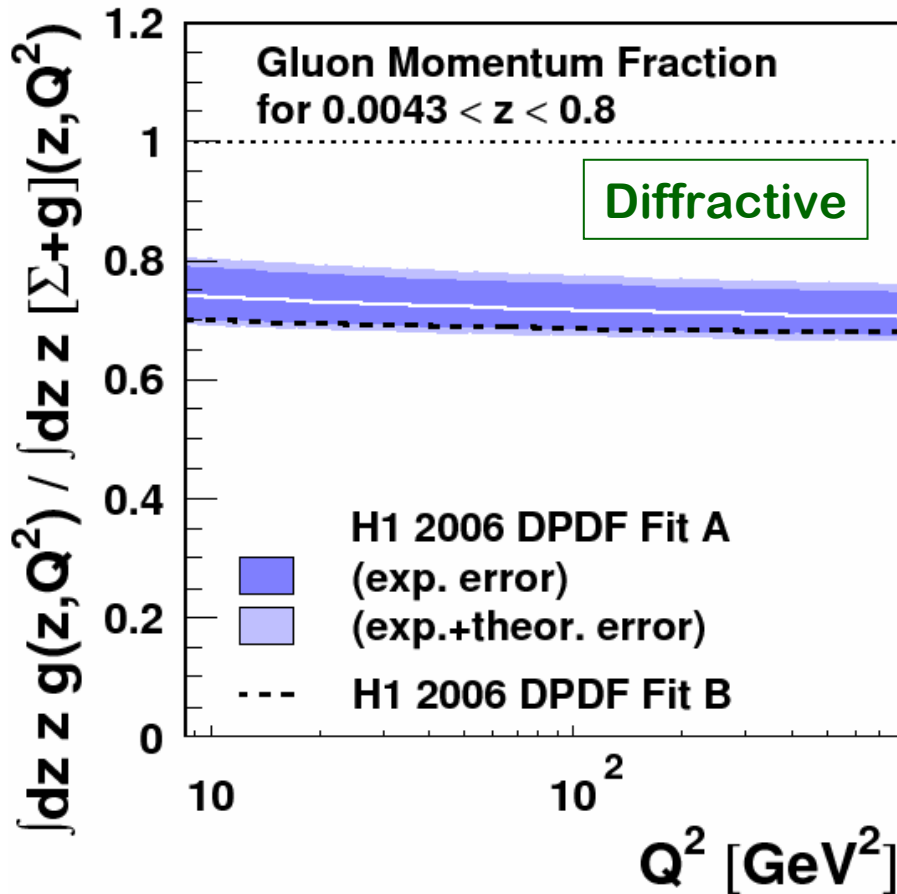
- Make ratio at fixed x_{IP} and x and fit it to $A+B \ln Q^2$



- Ratio remarkably flat (derivative ~ 0) except at high β

Q² derivative and gluon/quark ratios

- If $\frac{d(\sigma_r^D/\sigma_r)}{d \ln Q^2} \sim 0$ then $\frac{1}{\sigma_r^D} \frac{d\sigma_r^D}{d \ln Q^2} \approx \frac{1}{\sigma_r} \frac{d\sigma_r}{d \ln Q^2} \rightarrow \frac{g^D}{q^D} \sim \frac{g}{q}$



At low x, quark:gluon ratio $\sim 70\%/30\%$, common to diffractive and inclusive

Ratio diffractive/inclusive: x dependence

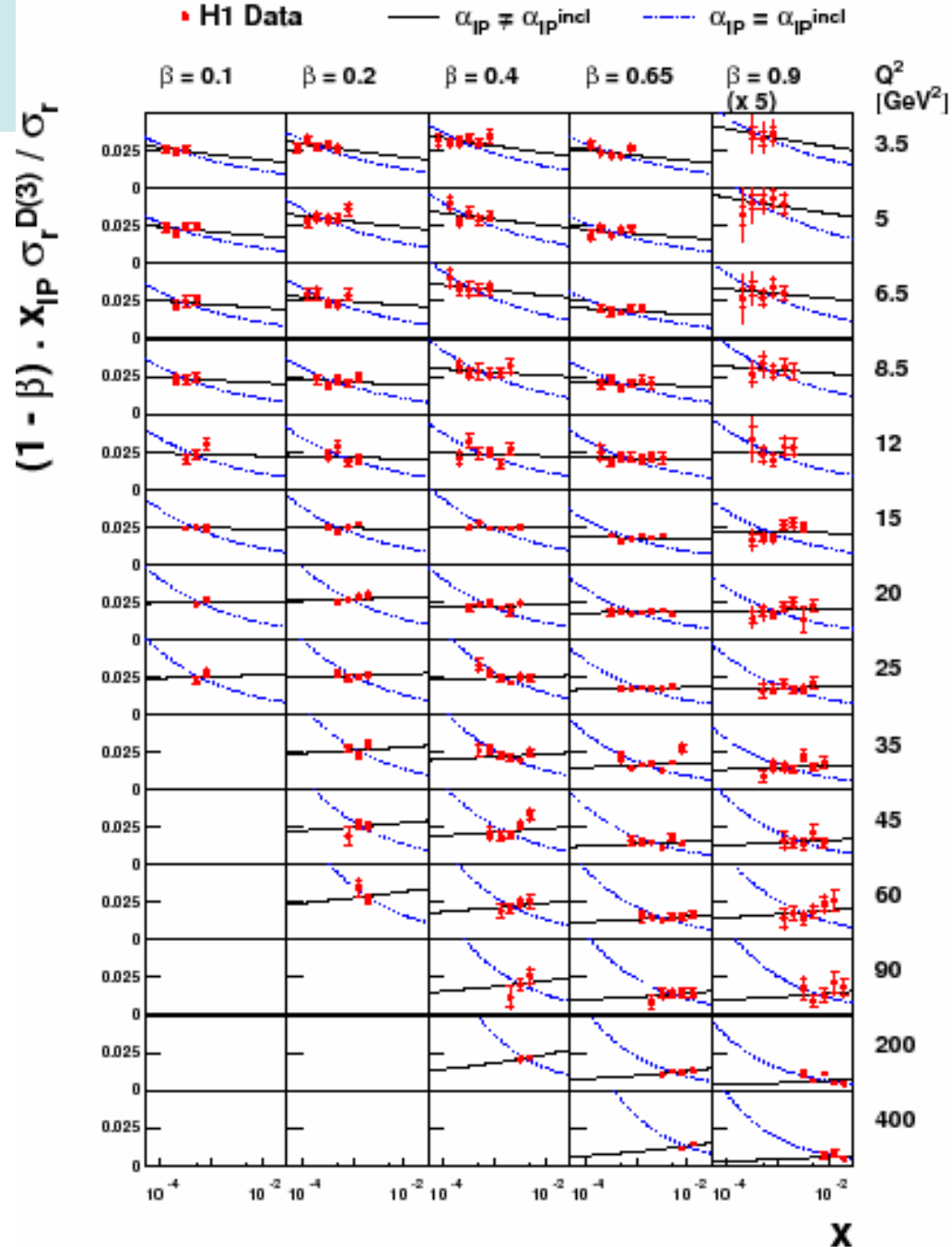
- Plot σ_r^D/σ_r at fixed β, Q^2 (hence fixed M_X) vs x ($\sim 1/W^2$)

- Corresponds to

$$M_X^2 \cdot \frac{d\sigma_r^D}{dM_X^2} / \sigma_{tot}$$

- Remarkably flat vs x over most of kinematic range (bins with large F_L or IR contrib not shown)

- Diffractive and inclusive cross sections cannot be described with the same $\alpha_{IP}(0)$, even if it is Q^2 dependent

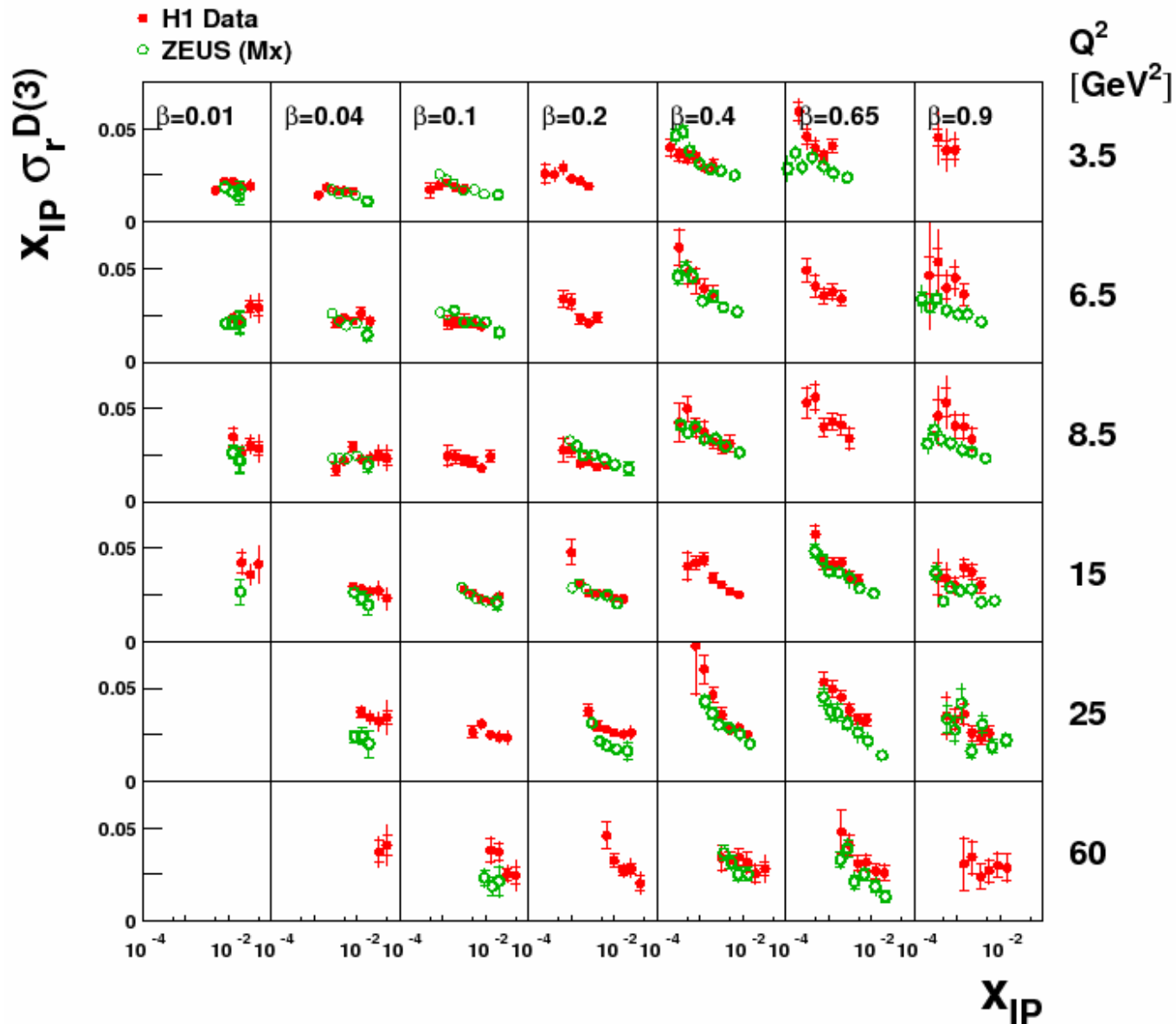


Summary

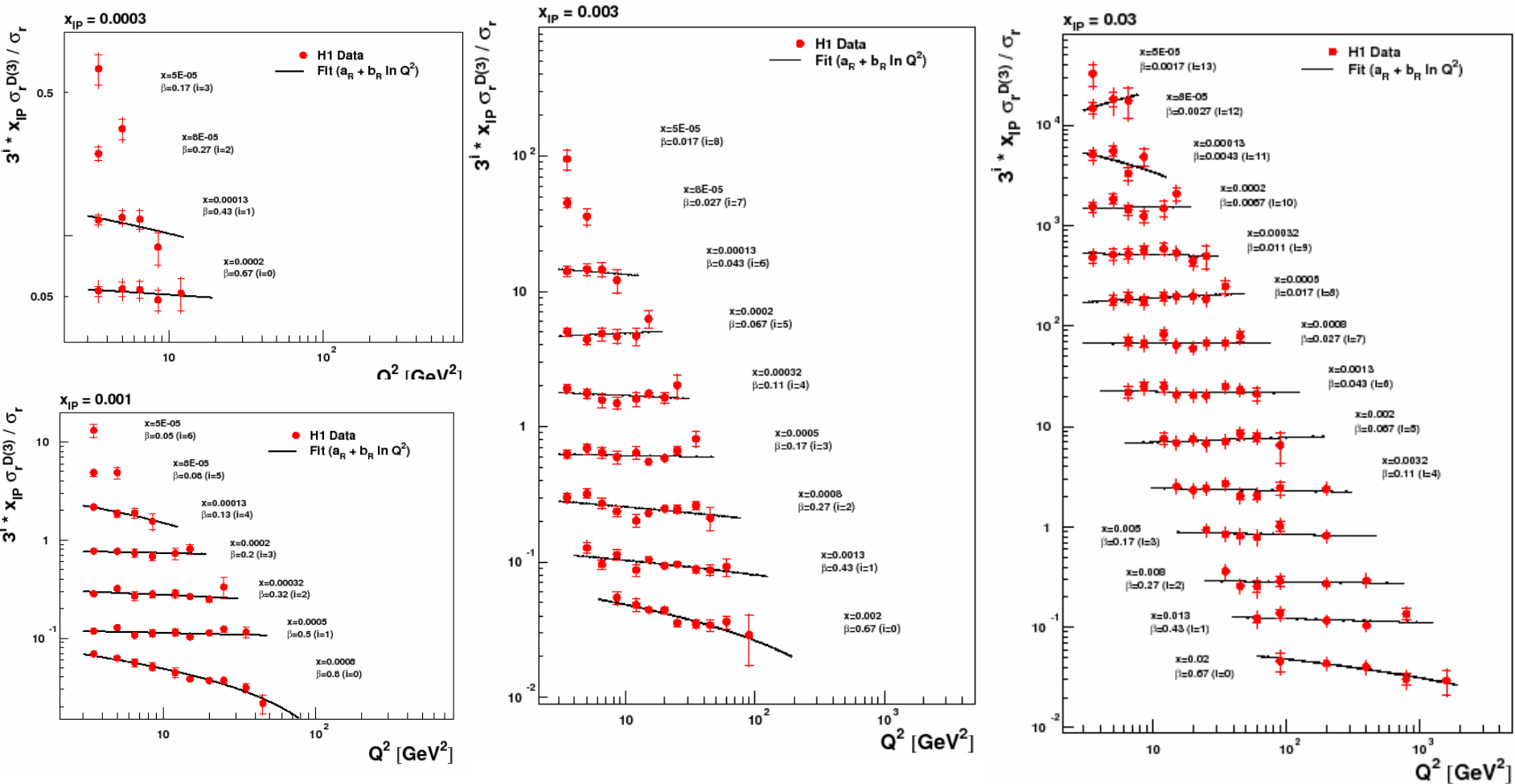
- H1 diffractive measurements using FPS and LRG methods published last week:
 - FPS method: DESY 06-048, hep-ex/0606003, subm. to EPJC
 - LRG method+QCD fits: DESY 06-049, hep-ex/0606004, subm. to EPJC
- Data from two methods agree in detail
- Slope parameter $B \sim 6 \text{ GeV}^{-2}$ at low x_{IP} , indep. of $x_{\text{IP}}, \beta, Q^2$
- Proton vtx factorization with reggeon exchanges at high x_{IP} continues to provide good model for x_{IP} dependence: $\alpha_{\text{IP}}(t) \sim 0.118 + 0.06 t$
- Diffractive PDFs extracted from fits to β, Q^2 dependences for $Q^2 \geq 8.5 \text{ GeV}^2$ (H1 2006 DPDF Fits A+B)
 - Quark singlet very well constrained ($\sim 5\%$)
 - Gluon constrained to $\sim 15\%$, but poorly known at high z
- DPDFs predict charged current cross sections OK
 - More comparisons with jets, charm etc. to follow
- Ratio diffractive/inclusive DIS measured
 - \sim flat with Q^2 at fixed x, x_{IP}
 - \sim flat with W at fixed Q^2, M_x

Extra Figures

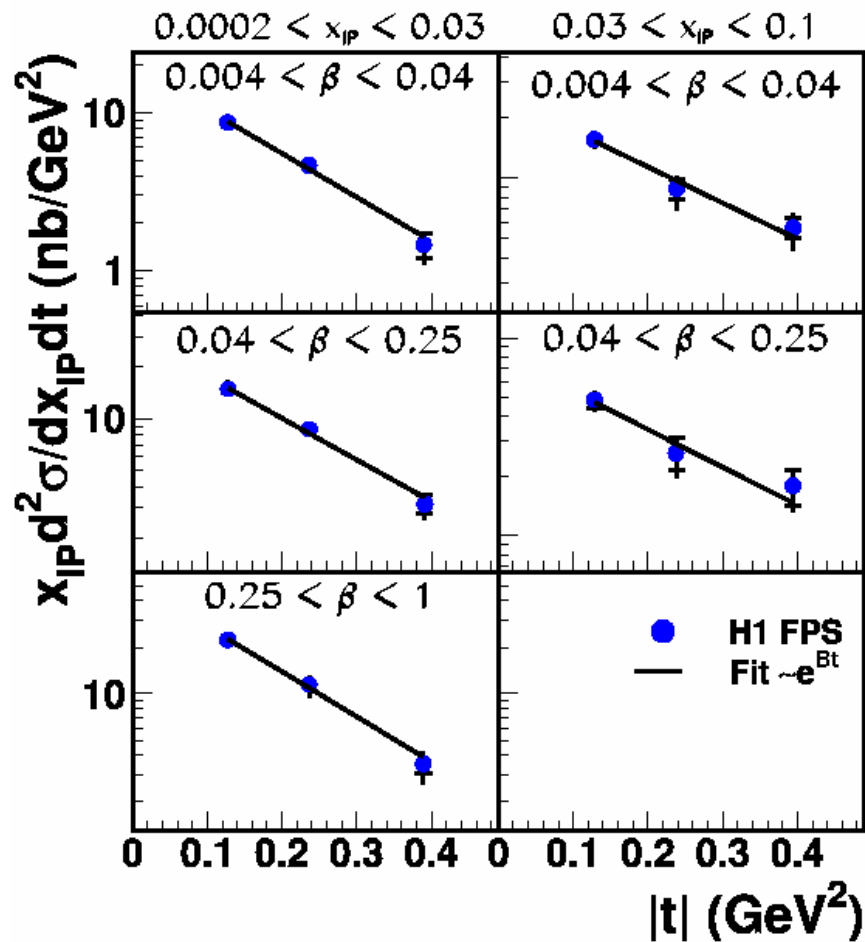
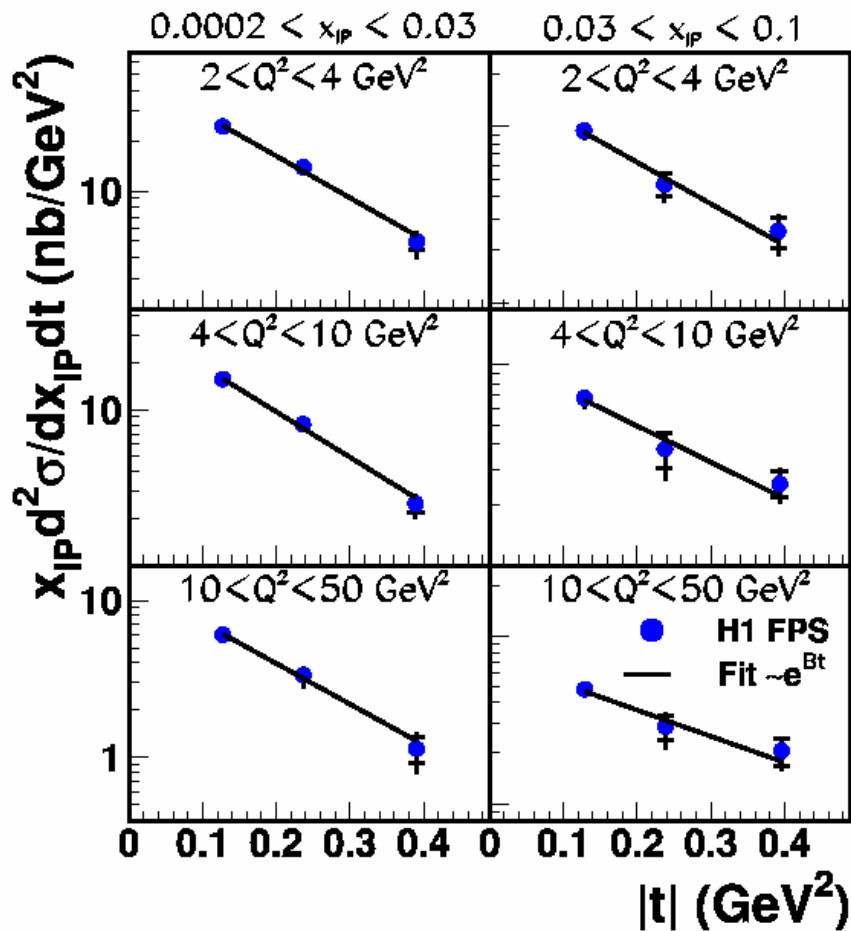
Comparison H1-LRG and ZEUS-Mx data



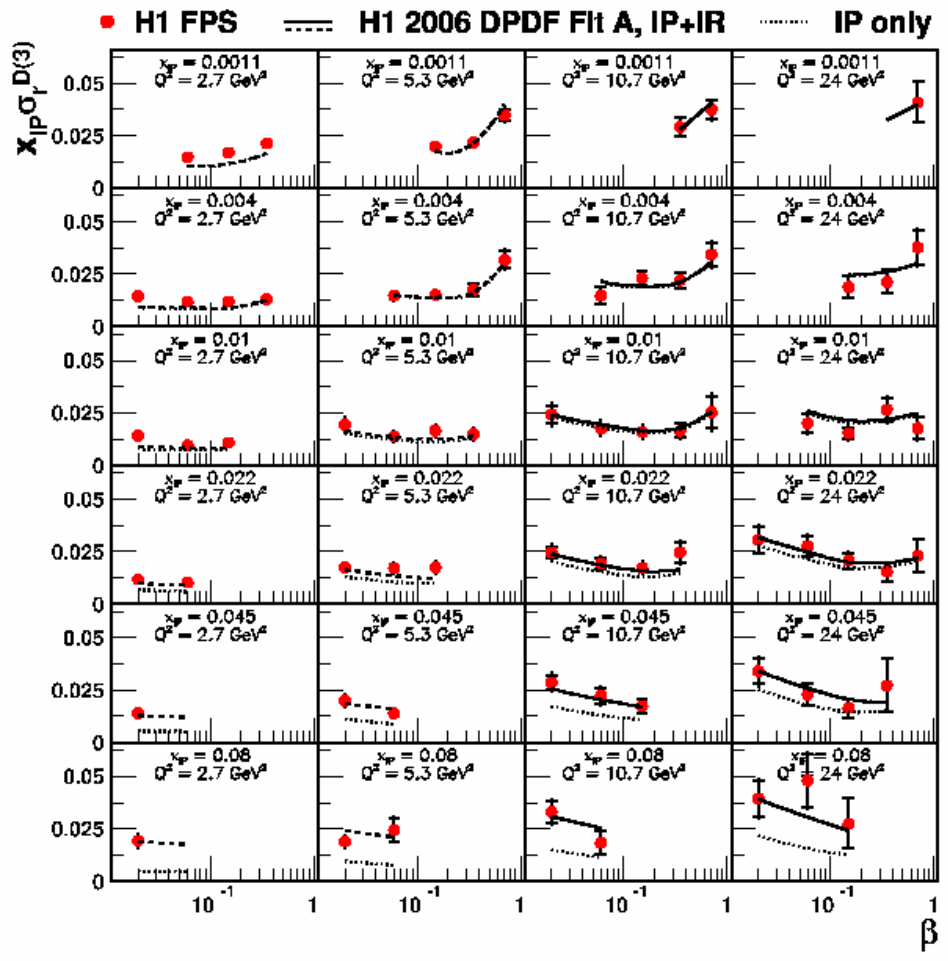
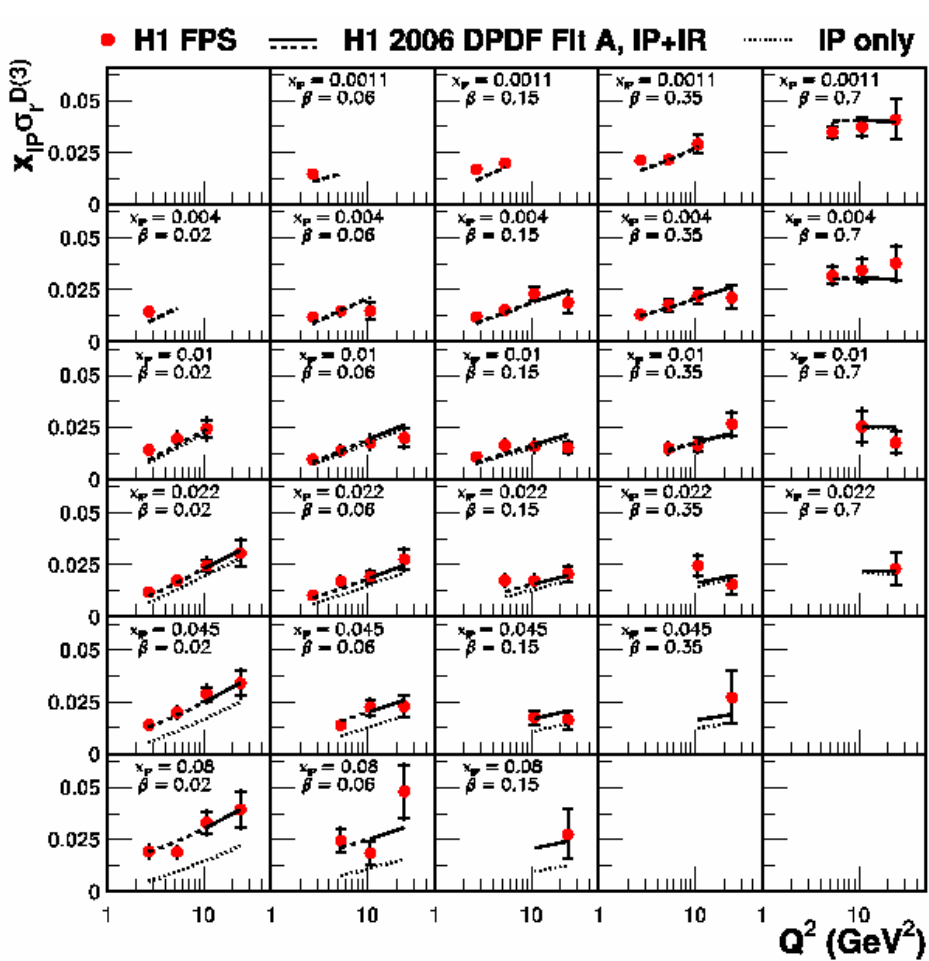
Ratio diffractive/inclusive vs Q^2 extra plots



t dependence in bins of β or Q^2



Q^2 and β dependences of FPS data



x_{IP} dependence of FPS data

